12-31-1991

Liquid-liquid dispersion in agitated vessels provided with multiple impellers

Yu-Tsang Huang
New Jersey Institute of Technology

Liquid-Liquid Dispersion in Agitated Vessels Provided with Multiple Impellers

by

Yu-Tsang Huang

Thesis submitted to the Faculty of the Graduate School of
the New Jersey Institute of Technology
in partial fulfillment of the requirement for the degree of
Master of Science in Chemical Engineering
December 1991

Abstract

Baffled vessels with multiple impellers are widely used in industry to generate liquid-liquid dispersions. In this work, a new method to determine the minimum agitation speed for complete dispersion in two immiscible liquids was developed. This method was conceived to replace the traditional visual observation method that has been extensively used in the past for this purpose. The minimum agitation speeds for liquid-liquid dispersion with single and multiple impellers in baffled vessel were also measured. The effect of a number of variables such as size and type of impellers, size of tank, impeller location, spacing between impellers, and dispersed phase volume fraction were studied. The results obtained in this work indicate that, contrary to intuition, the presence of multiple impellers may not necessarily be beneficial to the achievement of the just dispersed state for liquid-liquid dispersion. When a multiple impeller system was used the configuration with pitched blade turbines (pumping upward) required to least amount of power to produce a complete liquid-liquid dispersion.

APPROVAL

Title of Thesis:

Liquid-Liquid Dispersion in Agitated Vessels Provided with Multiple Impellers

Name of Candidate: Yu-Tsang Huang

Thesis and Abstract Approved:

Dr. Piero M. Armenante Date

Department of Chemical Engineering

Signatures of Other Members of the Thesis Committee:

Dr. Dana E. Knox Date

Department of Chemical Engineering

Dr. Robert Barat Date

Department of Chemical Engineering

Vita

Name: Yu-Tsang Huang

Permanent address:

Degree and date to be conferred: Master of Science, 1991

Date of birth:

Place of birth:

College Institutions	Degree	Date of Degree Attended
National Tsing Hua U., Taiwan	B.S.	June, 1987
New Jersey Inst. of Tech.	M.S.	December, 1991

Major: Chemical Engineering

ACKNOWLEDGEMENT

I wish to express my appreciation to all the people who contributed my research and thesis. I am thankful to each of my committee members, Dr. E. Knox and Dr. Robert Barat, for their useful suggestions and contributions. My thesis advisor Dr. Piero M. Armenante deserves a very special acknowledgement for his guidance, patience, and encouragement through the course of this study.

Finally, I want to thank all members of the Mixing Group who gave me needed support and suggestions during the research stage.

TABLE OF CONTENTS

TABLES

FIGURES

Chapter 1

Introduction

Liquid-liquid dispersions in baffled vessels provided with multiple impellers are widely used in industry. Some typical applications of these systems include solvent extraction, emulsion polymerization, and liquid membrane separation. The purpose of agitation is to produce as large as possible an interfacial area between the two immiscible phases, and therefore produce small droplets. In these processes, the agitation speed must be high enough to ensure complete dispersion of one liquid phase in the other immiscible phase. Therefore, it is of great interest to be able to predict the minimum agitation speed at which the complete dispersion state is achieved. Previous studies on the determination of the minimum agitation speed for liquid-liquid dispersion systems almost only considered one centrally mounted impeller. On the contrary, very few studies concerning two or multiple impellers systems can be found in the literature even though these systems are quite often used in industrial reactors.

The behavior of a liquid-liquid dispersion in baffled tanks with one or multiple impellers was also examined as a function of variables such as impeller type and diameter, impeller location, impeller number, distance between impellers, tank diameter, and volume fraction of the dispersed phase. In the present work, both a newly developed sampling method and the traditional visual observation method were used to determine the minimum agitation speed. The results obtained with multiple impellers systems were then compared with the results for single impeller systems.

Chapter 2

Literature Survey

2.1 Minimum Agitation Speed

Previous work on minimum agitation speed began with Nagata (1950), who used an unbaffled, flat-bottomed tank with a centrally mounted flat blade turbine with four blades (T/D=3, Ct/H=1/2, and blade width of 0.06T). Nagata obtained an empirical correlation for the minimum agitation speed, N_{cd}

$$N_{cd} = 6D^{-2/3} \left(\frac{\mu_c}{\rho_c}\right)^{1/9} \left(\frac{\rho_c - \rho_d}{\rho_c}\right)^{0.26} \tag{1}$$

He found no effect of interfacial tension on the minimum agitation speed. Van Heuven and Beek (1971) studied liquid dispersion with a six-blade disk turbine in a baffled vessel (D/T=1/3). They found

$$\frac{N_{cd}^2 D}{g} = 22\left(\frac{N_{cd} D^2}{\nu}\right)^{-3/5} \left(\frac{\rho \nu^2}{\sigma D}\right)^{-1/5} \left(\frac{\Delta\rho}{\rho}\right)(1 + 2.5\phi)^{7/3} \tag{2}$$

Rearrangement of Equation (2) resulted in

$$N_{cd} = \frac{3.28\, g^{0.38} \Delta\rho^{0.38} \mu_c^{0.08} \sigma^{0.08} (1 + 2.5\phi)^{0.9}}{D^{0.77} \rho^{0.54}} \tag{3}$$

Skelland and Seksaria (1978) studied the minimum agitation speed using four different types of impeller (propeller, pitched blade turbines, flat blade turbines, and curved turbines) in baffled vessels (H/T = 1, ϕ = 1/2, and T = constant). The variables they considered included location of impeller and liquid properties. In their study they also used two impellers mounted on the same shaft, but they did not consider the effect of impeller number and space between impellers on minimum agitation speed. Their correlation is given by

$$N_{cd} = C_0\, D^{\alpha_0}\, \mu_c^{1/9}\, \mu_d^{-1/9}\, \sigma^{0.3}\, \Delta\rho^{0.25} \qquad (4)$$

where C_0 and α_0 are dependent on the agitator geometry and the position of the agitator in the vessel (clearance distance).

Skelland and Ramsay (1987) combined the results of 251 runs from their own study with 35 experimental points obtained by van Heuven and Beek (1971) and 195 runs reported by Skelland and Seksaria (1978) to produce their correlation. The variables included 5 common types of impeller (3 radial and 2 axial flow) in 4 locations, fluid properties, tank diameter, impeller diameter, liquid height and volume fraction of dispersed phase. They obtained the following correlation

$$\frac{N_{cd}^2\, \rho_M\, D}{g\, \Delta\rho} = C^2 \left(\frac{T}{D}\right)^{2\alpha} \phi^{0.106} \left(\frac{\mu_M^2 \sigma}{D^5\, \rho_M\, g^2\, \Delta\rho^2}\right)^{0.084} \qquad (5)$$

where

$$\rho_M = \phi \rho_d + (1-\phi)\, \rho_c \qquad (6)$$

and

$$\mu_M = \frac{\mu_c}{1-\phi}\left(1 + \frac{1.5\, \mu_d\, \phi}{\mu_d + \mu_c}\right) \qquad (7)$$

Expansion of Equation 5 yields the expression

$$N_{cd} = C \left(\frac{T}{D}\right)^{\alpha} \left(\frac{g^{0.42}\, \Delta\rho^{0.42}\, \mu_M^{0.08}\, \rho^{0.04}\, \phi^{0.05}}{D^{0.71}\, \rho_M^{0.54}}\right) \tag{8}$$

The value of C and α are dependent on the type of impeller and its location. They compared Equation 8 with the correlation obtained by Zwietering (1958) for solid-liquid suspensions in a similar condition and obtained

$$N_{js} = C'\left(\frac{T}{D}\right)^{\alpha'} \frac{g^{0.45}\, \Delta\rho^{0.45}\, \mu_c^{0.1}\, D_p^{0.2}\, (100R)^{0.13}}{D^{0.85}\, \rho_c^{0.55}} \tag{9}$$

where C' and α' are constants based on impeller type and location.

It is interesting to notice the similarity between Equation 8 and Equation 9. This is consistent with the statement of van Heuven and Beek (1971) that a similar mechanism exists between complete liquid-liquid dispersion and solid-liquid dispersion.

Skelland and Ramsay's (1987) correlation (Equation 8) for the minimum agitation speed in liquid-liquid dispersion systems was used by Skelland and Moeti (1989) to predict the minimum agitation speed, when interfacial tension between the liquids was lowered by the presence of surface active agents. The overall deviation between the experimental data and their correlation was 11.67%. Skelland and Kanel (1990) also applied the same correlation to predict the minimum agitation speeds for non-Newtonian liquid-liquid dispersion systems. The overall absolute deviation was 8.9% for their 120 experimental points when Vermeulen *et al.*'s viscosity expression (1955) was combined with Metzner and Otto's definition of apparent viscosity (1957), μ_A, in place of μ.

No literature guidance exits, to the best of the author's knowledge, on minimum agitation speed for complete liquid-liquid dispersion when multiple impellers are used.

2.2 Power Consumption

In order to achieve the complete dispersion in two immiscible liquids it is necessary to apply energy and to transfer it to the liquid phases through the impellers. Rushton (1950) used dimensionless analysis to obtain a correlation for power consumption. He introduced the power number, N_p, defined as

$$N_p = \frac{P}{\rho N^3 D^5} \tag{10}$$

The relationship between power number and Reynolds number Re is

$$N_p = K\,(Re)^m \tag{11}$$

where the Reynolds number of a mixing system is defined as

$$Re = \frac{\rho N D^2}{\mu} \tag{12}$$

Depending on the Reynolds number, three zone can be distinguished:

$Re < 50$ laminar zone

$$N_p \propto \frac{1}{Re} \tag{13}$$

$50 < Re < 10^4$ transition zone, the power number is a function of the Reynolds number

$Re > 10^4$ fully turbulent zone, the power numbers are independent of the Reynolds number

The state of complete dispersion of two immiscible liquids in baffled vessels is typically associated with full turbulence. According to the study of van Heuven *et al.* (1971) for one six-blade disk turbine systems, the power number in this state was constant and the value was 5.4 ± 0.5.

Chapter 3

Experimental Apparatus and Method

3.1 Fluids Used.

Distilled water formed the continuous phase in all runs; the dispersed phase consisted one of the following fluids presaturated with water in all cases: mineral oil (ρ_d= 0.826g/cm^3) or heptane (ρ_d= 0.684g/cm^3).

3.2 Apparatus.

A schematic of the apparatus used in this work is shown in Figure 1. The experimental system consisted of a variable speed motor (Cole Parmer E650MG) with at a maximum speed of 3000 rpm. The agitation speed was measured using a digital tachometer with a photoelectric pick-up sensor (Cole Parmer) and was accurate within ± 1 rpm. The motor controller was provided with a power meter, which gave a reading proportional to the power delivered to the shaft. This meter was calibrated, as explained below in greater detail.

Three fully baffled cylindrical tanks were used. One tank was made of glass and provided with metal baffles secured to a ring placed above the tank. In this case, the baffle width was 8.7% of the tank diameter. The other two tanks were made entirely of Plexiglass. The dimensions of the tanks are given in Table 1a.

Three types of impellers namely disk turbines, flat blade turbines, and 45^0 pitch-blade turbines pumping either up or down (all available of three different sizes) were used, as shown in Figure 2. The shaft, impellers, and baffles were all made of 316 stainless steel. Depending on the experiment one, two, or three impellers were mounted on the shaft. The clearance of the lower impeller off the tank bottom, C_b or the clearance between top impeller and air-liquid interface, Ct and the spacing between the impellers (for the multiple impellers case), S, were varied during the experiments. Dimensions of the equipment are listed in Table 1b.

The sampling apparatus shown in Figure 1 consisted of a vertical glass tube 4 mm in internal diameter placed in the middle position between two baffles and at a radial distance from the shaft equal to the one half the tank radius. The distance of the sampling point from the tank bottom was varied. The sampling tube was connected to a series of flasks and hooked to a vacuum system. Several valves were used to divert the flow from the tank and through the sampling tube to either a reservoir or a graduated cylinder (25 mm in diameter, and 100 ml in volume).

3.3 Operational Method.

All equipment was washed with detergent, rinsed with distilled water, and air dried. Two immiscible liquids were poured into the tank. Depending on the experiment, the dispersed phase was from 10% to 30% by volume of the total liquid mixture, and the combined height of the liquids was always equal to the tank diameter. The motor was started at an agitation speed well below the minimum agitation speed for complete dispersion. After an equilibration period varying between 10 and 15 minutes the vacuum system was activated by opening Valve C (see Figure 1). Then, Valve A was opened so that the liquid would flow from the tank into the reservoir. This was done to insure that the material initially contained in the sampling tube would not be included in the sample. When some 50 ml of dispersion had accumulated in the reservoir Valve A was closed and Valve B was opened, thus allowing the flow to be diverted to the graduated cylinder until some 80 ml of dispersion were collected. The operation typically lasted only about 10 seconds. The last bottle in the line was added only to protect the vacuum system from accidently receiving some liquid. The mixture collected in the graduated cylinder was allowed to separate into two phases, and the fraction of the dispersed phase in the sample was determined. All the liquids were then returned to the tank. The same procedure was repeated at 5 to 11 different agitation speeds.

In addition, the minimum agitation speed for complete dispersion was also obtained in each experiment by visual inspection. Accordingly, N_{cd-vis}, the visually obtained value for N_{cd}, was defined as the minimum impeller speed at which no dispersed phase was observed at rest at the top of the continuous phase (Skelland and Seksaria, 1978). In most of our experiments we observed some hard-to-disperse small fluid pockets of approximately 1ml to 5ml near the baffle corners or around the impeller shaft. The presence of these pockets was neglected when N_{cd-vis} was determined since they were observed even at agitation speeds clearly associated with exceedingly well-mixed dispersion states. This approach is in line with the observations of previous investigators (Skelland and Seksaria, 1978; Godfrey *et al.*, 1984).

For each experiment the power consumption was read and recorded from the motor controller, which had been calibrated using an ELB agitator system (Chemineer). The calibration procedure consisted of reading and recording the power from the motor controller at predetermined constant agitation speeds for a given system, and using the ELB to measure the corresponding torques at the same speeds for the same system. Then the torques measured on the ELB were multiplied by the corresponding agitation speeds to give the power consumptions. A calibration plot of the power read from the motor controller against the power calculated from ELB was obtained. The calibration curve is shown in Figure 3.

Chapter 4

Result and Discussion

4.1 Determination of Minimum Agitation Speed Using the Sampling Method

The concentration of the dispersed phase in the samples, V*, was plotted as function of agitation speed (two examples were shown in Figure 4). From these plots one can see that a good estimate of N_{cd} can be obtained by just inspecting the plot and determining where the change in the slope occurs. While this method is unequivocal if a maximum exists, some arbitrariness can be introduced in cases such as that reported in Figure 4a, for which there is no maximum. This problem can be more serious, although not as significantly as in the visual method case, if the change in slope is not as pronounced.

In order to eliminate any ambiguity, we have developed a procedure that provides an unequivocal interpretation of the experimental plots. However, a distinction must be made between those plots that do not present a maximum vs. those which do.

Case 1. The plot of the experimental value of V* vs. N does not have any maxima

We used two methods to obtain a value for $N_{cd\text{-}smp}$ for the case in which no maxima are present. Both methods rely on the use of interpolating curves to produce a value for $N_{cd\text{-}smp}$. The first method is based on the use of a fourth-order polynomial, while the second uses spline curves.

Method 1a: the points are interpolated with a fourth-order polynomial

Each set of data points containing no maximum was fitted with a fourth order polynomial of the type:

$$V^* = a\,N^4 + b\,N^3 + c\,N^2 + d\,N + e = g\,(N) \qquad (14)$$

using the least square method, in order to obtain the values for the parameters a, b, c, d, and e. Then the value of $N_{cd\text{-}smp}$ was obtained by taking the third derivative of V* with respect to N and putting it equal to zero. Hence:

$$N_{cd\text{-}smp} = -\,b\,/\,(4a) \qquad (15)$$

The rationale for this method is the following. Assuming that the polynomial fits the points well, the first derivative of the polynomial gives the value of the slope of curve, the second derivative indicates the rate of change of the slope, and the hence the third derivative indicates how fast this rate of change is changing itself. Therefore, when an abrupt and significant drop in the positive but declining value of the slope occurs, as in correspondence of $N_{cd\text{-}vis}$, we can except to see a maximum rate of change of the slope, i.e., a minimum in the second derivative, and a corresponding zero of the third derivative. A pictorial representation of this process is shown in Figure 5.

Method 1b: The points are interpolated with spline curves

A second alternate method was devised to give a better correlation between $N_{cd\text{-}smp}$ and $N_{cd\text{-}vis}$. The same sets of data (with no maxima) used with the previous method were fitted this time with cubic spline curves. Then, from the function $V^* = f(N)$ so obtained, the function:

$$\phi(N) = \frac{f''(N)}{f'(N)} \qquad (16)$$

was derived, where $f'(N)$ and $f''(N)$ represent the first and second derivative of the interpolating spline curve function, respectively. The value for $N_{cd\text{-}smp}$ was obtained by imposing that:

$$\phi'(N) = 0$$

where $\phi'(N)$ is the derivative of $\phi(N)$. This time the rationale for the method is the following. The second derivative of the spline curve function $V^* = g(N)$ represents the rate of change of the slope, which appears to be greatest in correspondence of $N_{cd\text{-}vis}$. However, a better way to determine the point where the change is more signficant is by calculating the change in slope, i.e., $f''(N)$, with respect to the slope itself, $f'(N)$. The rate of change will be maximum (in absolute value) when the derivative of the function so derived, $\phi'(N)$, is zero. It should be remarked that the function $\phi(N)$ must be negative in correspondence of this point since the experimental points are increasing at a declining rate in the neighborhood of $N_{cd\text{-}vis}$. Figure 6 shows an example of the methodology used in this case.

Case 2. The plot of the experimental values of V* vs. N shows a maximum point

In this case, the simplest but still unequivocal determination of $N_{cd\text{-}smp}$ can be obtained by using that value of N within each appropriate data set for which V^* is maximum. However, we have found that a better way of interpreting the data is by fitting a series of spline curves through the experimental points and then taking the derivative of the resulting interpolating function and putting it equal to zero. The approach used in this case is illustrated in Figure 7.

A total of 65 experiments was conducted in which both N_{cd-vis} and N_{cd-smp} were determined for each experiment. Some experiments were conducted in triplicate to determine the reproducibility of the results for N_{cd-smp}. It was found that reproducibility was within 11.9%. Each value of N_{cd-smp} was obtained by generating a plot, such as those reported in the previous figures, containing some 5 to 11 experimental points. The plots that showed no maxima were roughly half of the total (32 out of 65). All the data are listed in Appendix A.

The plots that contained no maxima were first interpreted using Model 1a described above which utilized the fourth-order polynomial interpolation. A comparison between the values for N_{cd-vis} and N_{cd-smp} so obtained is shown in Figure 8. One can see that the agreement is, general speaking, rather good. However, some points are clearly off the 45^0 line. For this reason, the same "no-maxima" data were reanalyzed using the spline curve approach of Method 1b. The results are reported in Figure 9 (Remark: the number of points appearing in Figure 9 is greater than that of Figure 7 since the polynomial methods could not be reliably applied to all data set that contained too few points). One can see that the agreement is now much better across the entire range of values. When the points in this figure are fitted with a straight line using the least square method, the slope is 1.014 ± 0.038 (95% confidence interval), i.e., very close to the value of 1.0 that one would expect. The corresponding intercept is -1.17 ± 16 rpm and the coefficient of variation is 4.33%.

When we imposed to the regression line to pass through the origin, the slope was found to be 1.101. The standard deviation of the experimental data from the 45^0 degree line going through the origin was found to be 17.68 rpm with a coefficient of variation of 4.52%.

The plots containing maxima were analyzed as described above (Case 2), i.e., by determining the value of N in correspondence of the maximum point in the spline curves interpolated through the experimental points. The results are shown in Figure 10. Once again, the visually obtained values for the minimum agitation speed, $N_{cd\text{-}vis}$, compare very favorably with the values for $N_{cd\text{-}smp}$. A regression line through the points was found to have a slope of 0.990 $\pm$ 0.029 and an intercept of 1.61 $\pm$ 11.48 rpm (95% confidence interval in both cases). The correlation coefficient, standard error of estimate, and coefficient of variation were found to be 0.997, 13.059 rpm and 3.6%, respectively. It should be remarked that similar although not as good results were obtained even when the experimental maxima points from the plot were directly used without any interpolation. In such a case the error of the estimate was larger (26.69 rpm) and the correlation coefficient was only 0.987.

If the points in Figure 10 were interpolated with a straight line through the origin the slope was found to be 0.994. In addition, the standard deviation of the experimental points from the 45^0 degree line going through the origin was found to be 13.31 rpm with a coefficient of variation of 3.69%

Finally, all the points from the plots with or without maxima were combined together, as shown in Figure 11. In this figure the plots with no maxima were analyzed using the spline interpolation method (Method 1b). Also in this case the comparison between $N_{cd\text{-}vis}$ and $N_{cd\text{-}smp}$ appears to be quite favorable. The slope and intercept of a regression line through the points are 1.011 $\pm$ 0.024 and -4.39 $\pm$ 9.97 rpm, respectively. The correlation coefficient, standard error of the estimate, and coefficient of variation are 0.995, 15.82 rpm and 4.2%, respectively. If a straight line through the origin was considered the slope was found to be 1.0007. Finally, the standard deviation of the points from the 45^0 degree line through the origin was 15.93 rpm with a coefficient of variation of 4.24%.

4.2 Effect of Impeller Diameter on N_{cd} and Power Consumption

The effect of the impeller diameter on N_{cd} for systems having one, two or three impellers was studied. The results are shown in Figure 12. In Figure 12a, 12b, and 12c the clearance, Ct, between top impeller and the air-liquid interface was maintained constant, since the impeller closest to the dispersed phase was anticipated to have the greatest impact on achievement of the complete dispersed state. A regression of the experimental data produced the following results (all data and regression results were listed in Appendix B):

for disk turbines,

$N_{cd} \propto D^{-1.97}$ (for n=1, Ct = 7.6 cm) (17)

$N_{cd} \propto D^{-2.0}$ (for n=2, Ct = 7.6 cm) (18)

$N_{cd} \propto D^{-1.87}$ (for n=3, Ct = 7.6 cm) (19)

$N_{cd} \propto D^{-2.07}$ (for n=1, Ct = 9.4 cm) (20)

$N_{cd} \propto D^{-2.13}$ (for n=2, Ct = 9.4 cm) (21)

for flat blade turbines,

$N_{cd} \propto D^{-2.08}$ (for n=1, Ct = 8.4 cm) (22)

$N_{cd} \propto D^{-2.55}$ (for n=2, Ct = 8.4 cm) (23)

For the disk turbine case the number of impellers has little effect on the exponent of D, but for flat blade turbines this is not true. It is interesting to notice that as the clearance distance Ct increases, the value of the exponent also increases. This means that the relationship between impeller diameter and N_{cd} is also affected by Ct. The exponents found here compare well with those obtained by previous investigators. Skelland and

Ramsay (1987) found for one disk turbine systems the value of -2.41 ± 0.46 (Ct/T=1/2). For flat blade turbines the corresponding values are -2.09 ± 0.13 (Ct/T=1/2) and -2.73 ± 0.45 (Ct/T=3/4). The results obtained here compare favorably with the data obtained by Armenante, Mmbaga and Hemrajani (1991) for the case of floating solids. They found that for one impeller the exponent for D was -2.15 (for disk turbines, Ct/T=1/2) and -2.31 (for flat blade turbines, Ct/T=1/2).

Figure 12d shows the results obtained for the case in which the ratio Ct/D was kept constant. A regression of the data produced

for disk turbine

$N_{cd} \propto D^{-1\,94}$ (for n = 1, Ct/D = 1) (24)

$N_{cd} \propto D^{-1\,82}$ (for n = 2, Ct/D = 1) (25)

$N_{cd} \propto D^{-1\,47}$ (for n = 3, Ct/D = 1) (26)

These values are lower than those for the corresponding cases with constant Ct, and more similar to the value of -1.666 predicted by Tsai (1988) on the basis of Kolmogoroff's theory of isotropic turbulence.

Similarly, the total power consumption of the impeller(s) decreases as the impeller diameter is increased, but this relationship is strongly dependent on type of impellers and clearance distance.

4.3 Effect of Number of Impellers on N_{cd} and Power Consumption

The effect of the number of impellers, n, on the minimum agitation speed and power consumption at different spacings between impellers is shown in Figure 13 for three types of impellers. One can see that in most cases an increase in the number of impellers does not necessarily correspond to a reduction in the agitation speed for complete dispersion. Clearly the uppermost impeller in multiple impeller systems has the greatest effect on N_{cd}. For two-impeller systems the lower impeller also has an effect on N_{cd}, but not as much as the upper one. For three-impeller systems the lowest impeller has a negligible impact on N_{cd}. In some systems (Figure 12b and 12c) three impellers were actually worse than two impellers, as far as N_{cd} is concerned. It could be that the presence of the additional impeller results in a flow pattern interfering with the flow pattern of the other impellers. As the space between the impellers is increased, this effect becomes more significant.

The power consumption to achieve the complete dispersion state was found to be higher for the multiple impeller cases than for the single impeller cases. The only exception was the dual flat blade turbine systems.

4.4 Effect of Tank Diameter on N_{cd} and Power Consumption

The effect of tank diameter was studied in two ways. In a first set of experiments Ct/T was kept constant. In a second set of experiments Ct/D was maintained constant. Three different tank sizes (18.9 cm, 24.6 cm, 28.6 cm in diameter) were used in both sets. The results are shown in Figure 14 and Figure 15. From Figure 14 the following relationships were obtained:

for disk turbines

$$N_{cd} \propto T^{1.24} \quad (n=1,\ Ct/T = 0.31) \qquad (27)$$

$$N_{cd} \propto T^{1.35} \quad (n=2,\ Ct/T = 0.31) \qquad (28)$$

$$N_{cd} \propto T^{1.03} \quad (n=3,\ Ct/T = 0.31) \qquad (29)$$

for flat blade turbines

$$N_{cd} \propto T^{1.45} \quad (n=1,\ Ct/T = 0.31) \qquad (30)$$

$$N_{cd} \propto T^{1.38} \quad (n=2,\ Ct/T = 0.31) \qquad (31)$$

$$N_{cd} \propto T^{1.29} \quad (n=3,\ Ct/T = 0.31) \qquad (32)$$

for pitched blade turbines

$$N_{cd} \propto T^{1.17} \quad (n=1,\ Ct/T = 0.31) \qquad (33)$$

$$N_{cd} \propto T^{1.23} \quad (n=2,\ Ct/T = 0.31) \qquad (34)$$

$$N_{cd} \propto T^{0.54} \quad (n=3,\ Ct/T = 0.31) \qquad (35)$$

For the same type of impellers the value of the exponents for T are similar. The regression coefficients for these correlations are close to 1 except for the case of the three pitched blade turbine system (only 0.852). A comparison of these data with the data obtained by Skelland and Ramsay (1987) [1.70 $\pm$ 0.45 for one disk turbine (Ct/T=1/2), 1.38 $\pm$ 0.13 for one flat blade turbine (Ct/T=1/2), and 1.17 $\pm$ 0.47 for one pitched blade turbine (Ct/T=3/4)] shows that the results are similar. However, in the second set of experiments (shown in Figure 15) in which Ct/D were kept constant the results were more complex than the first case and the regression data are:

for disk turbines

$$N_{cd} \propto T^{1.03} \quad (n=1,\ Ct/D = 1) \tag{36}$$

$$N_{cd} \propto T^{0.37} \quad (n=2,\ Ct/D = 1) \tag{37}$$

$$N_{cd} \propto T^{0.37} \quad (n=3,\ Ct/D = 1) \tag{38}$$

for flat blade turbines

$$N_{cd} \propto T^{0.18} \quad (n=1,\ Ct/D = 1) \tag{39}$$

$$N_{cd} \propto T^{0.24} \quad (n=2,\ Ct/D = 1) \tag{40}$$

$$N_{cd} \propto T^{-0.25} \quad (n=3,\ Ct/D = 1) \tag{41}$$

for pitched blade turbines

$$N_{cd} \propto T^{0.08} \quad (n=1,\ Ct/D = 1) \tag{42}$$

$$N_{cd} \propto T^{-0.11} \quad (n=2,\ Ct/D = 1) \tag{43}$$

$$N_{cd} \propto T^{0.10} \quad (n=3,\ Ct/D = 1) \tag{44}$$

The effect of tank diameter on power consumption is strongly dependent on the type of impellers and clearance distance. In general, for all types of impellers the power consumption increases with the tank diameter as Ct/T is kept constant. However, for the case, constant Ct/D, the effect is more complex.

4.5 Effect of Volume Fraction of Dispersed Phase on N_{cd} and Power Consumption

The effect of volume fraction of dispersed phase on minimum agitation speed for liquid dispersion is shown in Figure 16. From this figure one can see the minimum agitation speed for liquid-liquid dispersion is weakly dependent on the volume fraction. This relationship is similar to that reported previously for similar systems (Mersmann *et al.*, 1982). In our work we also found that an increasing volume fraction of the dispersed phase lead to an increase of the mean drop size of dispersed liquid. This result was obtained by visual inspection of the mixture. However, no drop size measurements were made. This result is agreement with previous studies by van Heuven (1971) and Okufi *et al.* (1990). For one impeller systems, the value for the exponent of ϕ obtained by Skelland and Ramsay was 0.05. Our results are 0.01, 0.04, and 0.07 for disk turbine, flat blade, pitched blade turbine, respectively. For multiple impeller systems the results are more complicated.

From Figure 17 one can see that the effect of the volume fraction of the dispersed phase on power consumption is very complicated. We can only see that pitched blade turbines consume less power than the other two types of impeller to achieve the complete dispersion state.

4.6 Effect of Clearance Distance on N_{cd} and Power Consumption

The effect of the clearance between the air-liquid interface and the top impeller on minimum agitation speed was significantly complex, as shown in Figure 18. Very few previous studies considered this effect. Although some literature concerning the effect of clearance distance on minimum suspension speed for the solid-liquid system can be found (Raghava Rao *et al.* 1988), no correlations on this effect have been produced. For small values of Ct the presence of multiple impellers has some effect on N_{cd}. As Ct is increased the effect is reduced. This phenomena can be explained by noticing that the flow pattern of the lower impeller(s) interferes with that of the upper impeller.

The power consumption is also significantly affected by the clearance distance. For multiple impellers systems, as Ct is increased from T/3 to T/2, the power consumption increases sharply.

4.7 Effect of Spacing Between Impellers on N_{cd} and Power Consumption

The effect of the spacing between impellers, S, was considered at constant Ct/D as shown in Figure 19. For two impellers mounted on the central shaft the results are show in Figure 19a and can be correlated by the following equations:

$N_{cd} \propto S^{0.10}$ (for 2 disk turbines) (45)

$N_{cd} \propto S^{0.27}$ (for 2 flat blade turbines) (46)

$N_{cd} \propto S^{0.14}$ (for 2 pitched blade turbines) (47)

For three impellers the results were

$N_{cd} \propto S^{0.01}$ (for 3 disk turbines) (48)

$N_{cd} \propto S^{0.41}$ (for 3 flat blade turbines) (49)

$N_{cd} \propto S^{0.21}$ (for 3 pitched blade turbines) (50)

The effect of S on power consumption is more significant than on N_{cd}. For two-impeller systems there are a sharp changes in the range $1 < S/D < 1.4$. This result is compatible with the study of Armenante, Li, and Huang (1991) for solid-liquid suspension in multiple impeller systems.

Chapter 5

Conclusions

1. The results found in this work justify the claim that the minimum agitation speed for the complete dispersion of two immiscible liquids in mechanically agitated vessels can be experimentally obtained by plotting the volume fraction of the dispersed phase from samples taken from the vessel vs. the corresponding agitation speed.

2. The effects of impeller diameter or tank diameter on minimum agitation speed is similar for single impeller and multiple impeller systems. The exponent values of D in N_{cd} vs. D increase with an increase in clearance between the upper impeller and the air-liquid surface.

3. The use of multiple impellers may not be advantageous to the achievement of the minimum agitation state for liquid-liquid dispersion. In general, the minimum agitation speed is only slightly affected by the presence of the additional impeller. However, if the flow pattern of the additional impellers contrasts with the flow pattern established by a single impeller then the minimum agitation speed for the multiple impellers may be higher than the state for one impeller system.

In addition, the power consumption in correspondence of the minimum agitation for complete dispersion was generally found to be higher for multiple impeller cases than for the single impeller cases.

NOMENCLATURE

a	Parameter in Equation 1; rpm-4
b	Parameter in Equation 2; rpm-3
c	Parameter in Equation 3; rpm-2
C, C_0, C'	Constants
d	Parameter in Equation 4; rpm-1
e	Parameter in Equation 1; non-dimensional
Ct	Distance between the impeller and the air liquid interface; m or cm
Cb	Distance between the impeller and the bottom of vessel; m or cm
D	Impeller diameter; m or cm
H	Height of liquid in the vessel; m or cm
n	Number of impellers mounted on the same shaft, non-dimensional
m	Constant
N	Agitation speed; revolutions per minute (rpm)
f(N)	Spline curve interpolation function correlating the experimental values of V* with the corresponding values of N; non-dimensional
g(N)	fourth-order interpolation function correlating the experimental values of V* with the corresponding values of N; non-dimensional
N_{cd}	Minimum agitation speed for complete dispersion in liquid-liquid systems; revolutions per minute (rpm)
N_{cd-vis}	Minimum agitation speed for complete dispersion in liquid-liquid systems using the visual method; revolutions per minute (rpm)
N_{cd-smp}	Minimum agitation speed for complete dispersion in liquid-liquid systems using the sampling method; revolutions per minute (rpm)

N_{js} Minimum agitation speed for complete suspension of solid particles in liquid; revolution per minute (rpm)

N_p Power number $(\frac{P}{\rho N^3 D^5})$

P Power input to the system; watts

R Weight fraction of solids

Re Reynolds number $(\frac{\rho N D^2}{\mu})$

S Distance of between impellers; cm

T Vessel diameter; m or cm

V* Ratio of dispersed phase volume in sample to total sample volume; non-dimensional

Greek Symbols

α, α_0, α' Constants

ϕ Volume fraction of dispersed phase

ϕ(N) Ratio of second derivative of f(N) to first derivative of f(N); non-dimensional

μ_A Apparent viscosity for agitation corresponding to $(du/dy)_A$; kg/m sec

μ_C Viscosity of continuous phase; Ns/m^3

μ_M Defined by Equation 7; Ns/m^2

ρ_C Density of continuous phase; kg/m^3

ρ_d Density of dispersed liquid; kg/m^3 or g/cm^3

ρ_M Defined by Equation 6; kg/m^3

σ interfacial tension; $kg/_{sec}2$

ν Kinematic viscosity of the continuous phase (m_C/ρ); cm^2/sec

REFERENCES

Armenante, P. M., Mmbaga, J. P., and Hemrajani, R. R., 1991, Mechanism for the Entrainment of Floating Particles in Mechanically Agitated Liquids, *Proc. 7th Europ. Conf. on Mixing*, Brugge, Belgium, 18-20 Sept. 1991, Vol. 2, 555-564.

Armenante, P. M., Huang, Y. T., and Li, T., 1991, Determination of the Minimum Agitation Speed to Attain the Just Dispersed State in Solid-Liquid and Liquid-Liquid Reactors Provided With Multiple Impellers, Submitted to *Chem. Eng. Sci.*, Dec. 1991.

Godfrey J. C., Reeve R. N., and Grilc V., 1984, Minimum Conditions for the Production of Liquid-Liquid Dispersions in Agitated Tanks, *Inst. Chem. Eng. Symp.* Ser., **89**, 107-126.

Mersmann, A. and Grossman, H., 1982, Dispersion of Immiscible Liquids in Agitated Vessels. *International Chemical Engineering*, (Germany). Vol. 22, No 4, 581-590.

Metzner, A. B. and Otto, R. E. 1957, Agitation of Non-Newtonian Fluids, *AIChE J.* **3**(1), 3-10.

Nagata S., 1950. Studied on Agitation of two Immiscible Liquids, *Trans. Soc. Chem. Eng*. Japan, **8**, 43-58.

Okufi, S., Peree de Ortie , E. S., Sawistowski, H., 1990, Scale-up of Liquid-Liquid Dispersions in Stirred Tanks, *J Chem. Eng of Can*. **68**, 400-406.

Oldshue, J. Y. 1983, "*Fluid Mixing Technology*", McGraw-Hill Pub.Co., New York, NY., p125-140

Pavlushenko, I. S. and Ianishevskii., 1958, Rotation Speeds of Stirrers in the Stirring of Two Mutually insoluble Liquids, *J. of Applied Chem. of the USSR.*, **31**, 1334-1340.

Raghava Rao, K. S. M. S., Rewatkar, V. B., Joshi, J. B., 1988, Critical Impeller Speed for Solid Suspension in Mechanically Agitated Container, *AIChE J.*, Vol. 34, No 8, 1322-1340

Rushton, J.H., Costich E. W. , Everett H. J., 1950, Power Characteristics of Mixing Impeller, *Chem. Eng. Progr.*, **46**, (395), 467

Skelland, A. H. P. and Kanel, J. S., 1990, Minimum impeller Speed for Complete Dispersion of Non-Newtonian Liquid-Liquid Systems in Baffled Vessels, *Ind. Eng. Chem. Res.*, **29**, 1300-1306.

Skelland, A. H. P. and Lee, J. M., 1978, Agitator Speed in Baffled Vessels for Uniform Liquid-Liquid Dispersions, *Ind. Eng. Chem. Process Des. Dev.*, **17**, 473-478.

Skelland, A. H. P. and Moeti, L. T., 1989, Effect of Surface Active Agents on Minimum Impeller Speed for Liquid-Liquid Dispersion in Baffled Vessels, *Ind. Eng. Chem. Res.*, **28**, 122-127.

Skelland, A. H. P. and Ramsey, G. G., 1987, Minimum Agitation Speed for Complete Liquid-Liquid Dispersion, *Ind. Eng. Chem. Res.*, **26**, 77-81.

Skelland A. H. P. and Seksaria, R., 1978, Minimum Impeller speeds for Liquid-Liquid Dispersion in Baffled Vessels, *Ind. Eng. Chem. Process Dev.*, **17**, 56-61.

Tsai, D. H., Agitation Requirements for Complete Dispersion of Emulsions, M.S. Thesis, 1988, N.J.I.T., Newark, NJ.

van Heuven, J. W. and Beek, W. J., 1971, Power Input, Drop Size and Minimum Stirrer Speed for Liquid-Liquid Dispersions in Stirred Tanks, *Proceeding ISEC*, Paper 51, 70-81.

Vermeulen, T., Willians, G. M., Langlosis, G. E., 1955, Interfacial Area in Liquid-Liquid and Gas-Liquid Agitation, *Chem. Eng. Prog.*, **51** (2), 85F-94F.

Zwietering T. N. 1958, Suspension of Solid Particles in Liquid by Agitator, *Chem. Eng. Sci.*, **8**, 224-253.

Table 1. Apparatus Dimensions

1a. Dimensions of Tanks (cm)

material of construction	Plexiglass	Plexiglass	Glass
internal diameter of vessel	18.9	24.6	28.6
height of liquid	18.9	24.6	28.6
height of vessel	23.1	33.1	46.0
baffle width	2.0	2.0	2.5
baffle thickness	0.6	0.6	0.3

1b. Dimensions of Impellers (cm)

diameter of shaft	1.2		
diameter of disk turbine	6.4	7.6	10.2
diameter of flat blade turbine	6.4	7.6	10.2
diameter of pitched blade turbine	6.4	7.6	
width of disk turbine	1.2	1.5	2.0
width of flat blade turbine	0.8	0.9	1.2
width of pitched blade turbine	0.9	1.2	

Figure Caption

Figure 1. Experimental apparatus

Figure 2. Types of impellers

Figure 3. Calibration curve for power reading

Figure 4. Examples of experimental plots of volume fraction of dispersed phase, V*, vs. agitation speed, N, (a.) Plot not containing a maximum point (system: 10% heptane in water, 2 flat blade turbines, H = T = 28.6 cm, D = 10.2 cm, Cb = 8 cm, S = 10 cm, sampling location from vessel bottom: 10 cm); (b.) Plot containing a maximum point (system: 10% oil in water, 1 disk turbine, H = T = 24.6 cm, D = 7.6 cm, Cb = 10.2 cm, sampling location from vessel bottom: 11.4 cm)

Figure 5. Analysis of an experimental plot containing no maximum using Method 1a. (same experimental conditions as in Figure 4a) (a.) Experimental points; (b.) Interpolation curve using 4th order polynomial method; (c.) First and second derivative of interpolation curve; (d.) Third derivative of interpolation curve with Ncd-smp point.

Figure 6. Analysis of an experimental plot containing no maximum using Method 1b. (same experimental conditions as in Figure 4a) (a.) Experimental points; (b.) Interpolation curve using cubic spline method; (c.) Plot of f(N) vs. N; (d.) Plot of f'(N) vs. N.

Figure 7. Analysis of an experimental plot containing a maximum point. (same experimental conditions as in Figure 4b) (a.) Experimental points; (b.) Interpolation curve using cubic spline method; (c.) First derivative of interpolation curve with Ncd-smp point.

Figure 8. Comparison of $N_{cd\text{-}smp}$ with $N_{cd\text{-}vis}$ using Method 1a for experimental points whose plots do not contain any maximum point.

Figure 9. Comparison of $N_{cd\text{-}smp}$ with $N_{cd\text{-}vis}$ using Method 1b for experimental points whose plots do not contain any maximum point.

Figure 10. Comparison of $N_{cd\text{-}smp}$ with $N_{cd\text{-}vis}$ for experimental points whose plots contain a maximum point.

Figure 11. Comparison of $N_{cd\text{-}smp}$ with $N_{cd\text{-}vis}$ using all points.

Figure 12. Effect of impeller diameter on N_{cd} and power consumption. (a.), (b.), (c.): constant Ct; (d.): constant Ct/D.

Figure 13. Effect of number of impellers on N_{cd} and power consumption.

Figure 14. Effect of tank diameter on N_{cd} and power consumption.(constant Ct/T)

Figure 15. Effect of tank diameter on N_{cd} and power consumption.(constant Ct/D)

Figure 16. Effect of volume fraction of dispersed phase on N_{cd}.

Figure 17. Effect of volume fraction of dispersed phase on power consumption.

Figure 18. Effect of clearance distance on N_{cd} and power consumption.

Figure 19. Effect of spacing between impellers on N_{cd} and power consumption.

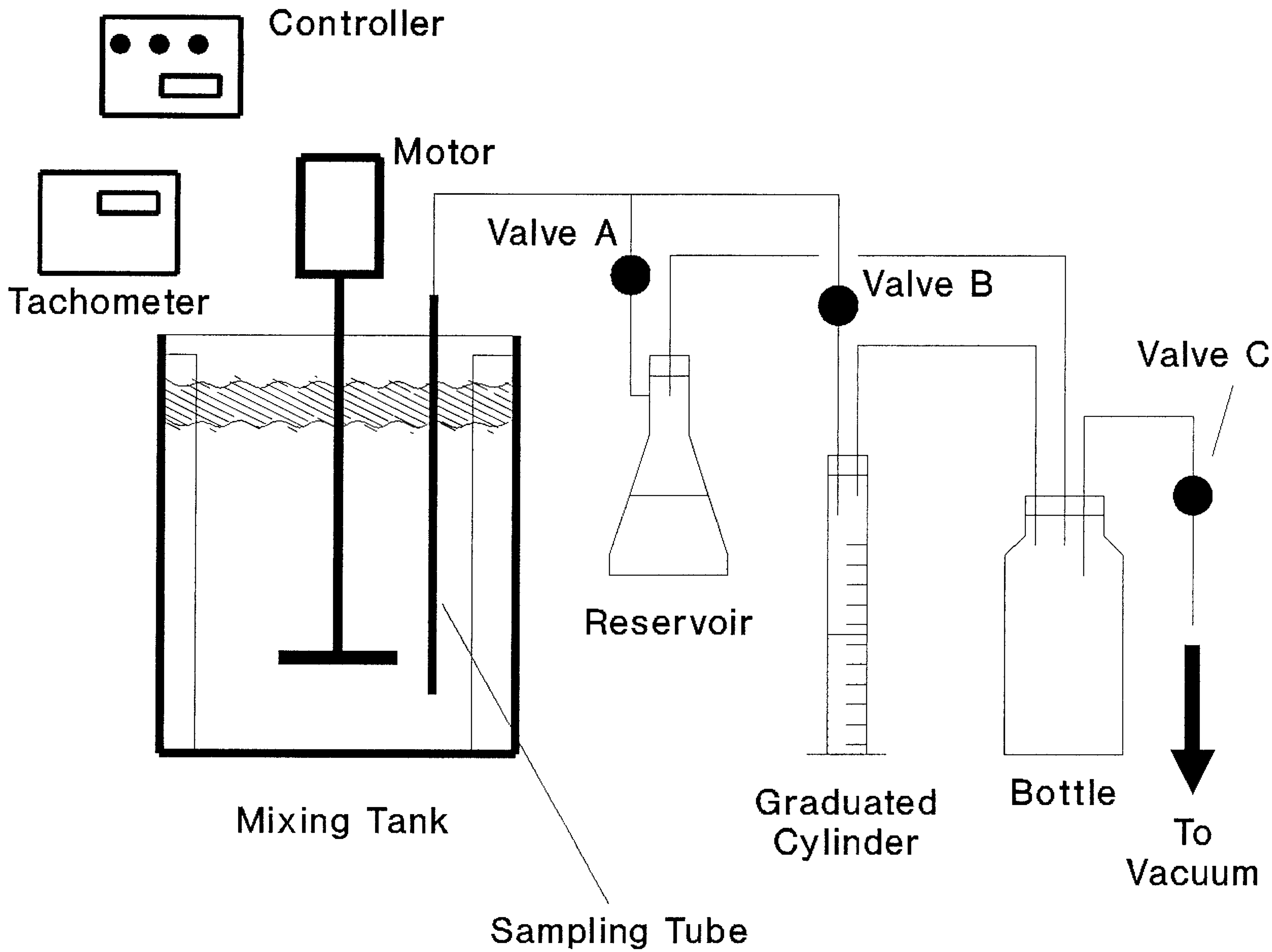
Controller
Tachometer
Motor
Valve A
Valve B
Valve C
Reservoir
Mixing Tank
Graduated Cylinder
Bottle
To Vacuum
Sampling Tube

Figure 1.

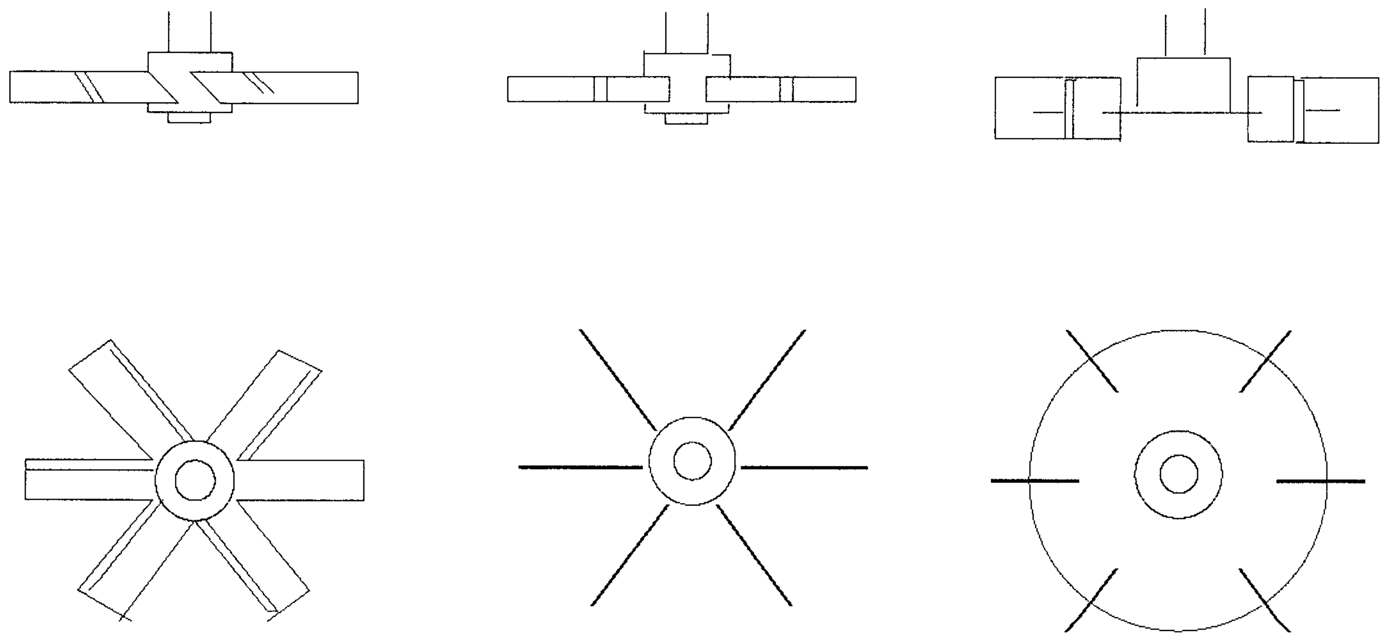

(a) Pitched blade turbine (b) Flat blade turbine (c) Disk turbine

Figure 2.

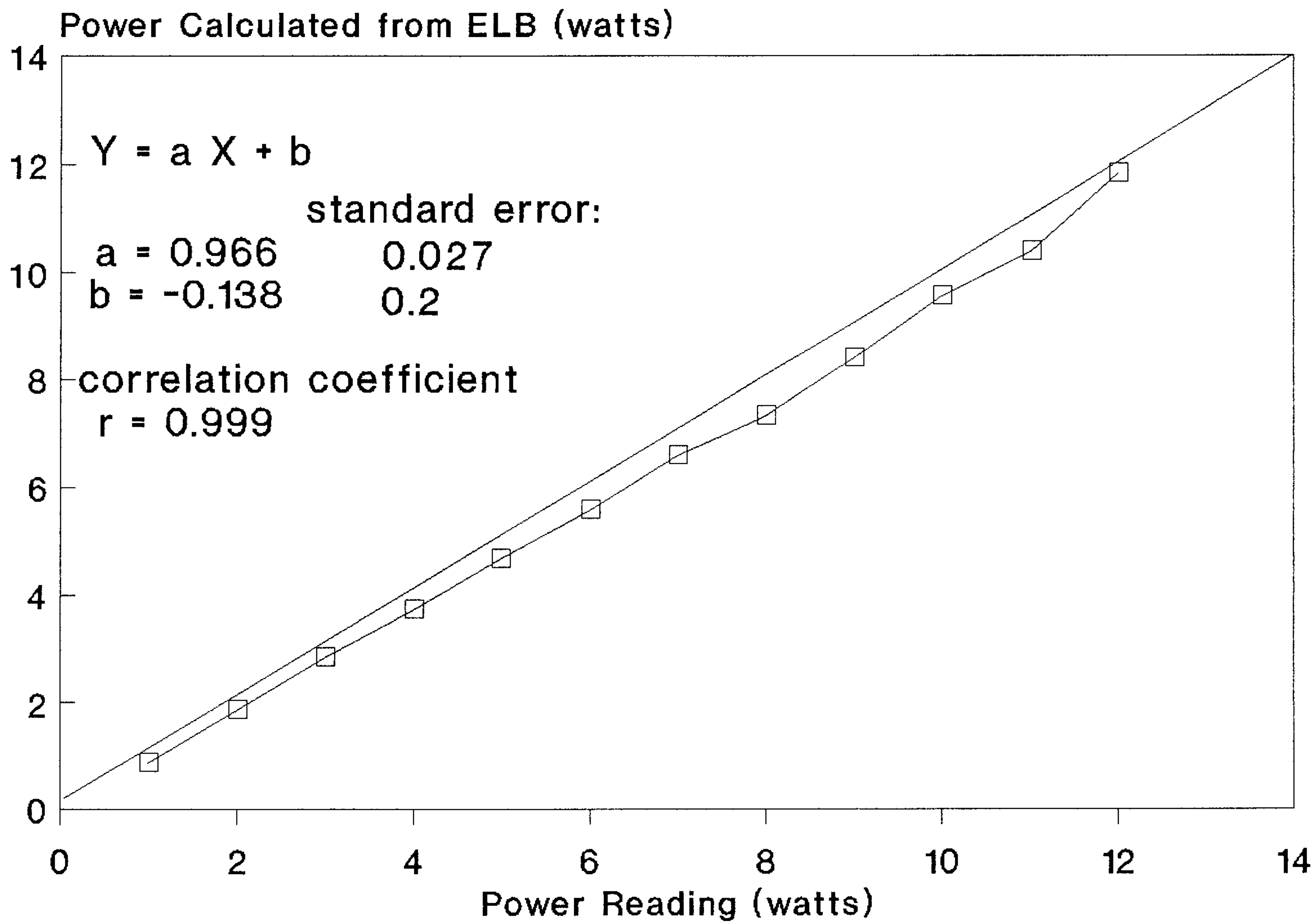
Power Calculated from ELB (watts)
Y = a X + b
standard error:
a = 0.966 0.027
b = -0.138 0.2
correlation coefficient
r = 0.999
0 2 4 6 8 10 12 14
0 2 4 6 8 10 12 14
Power Reading (watts)

Figure 3.

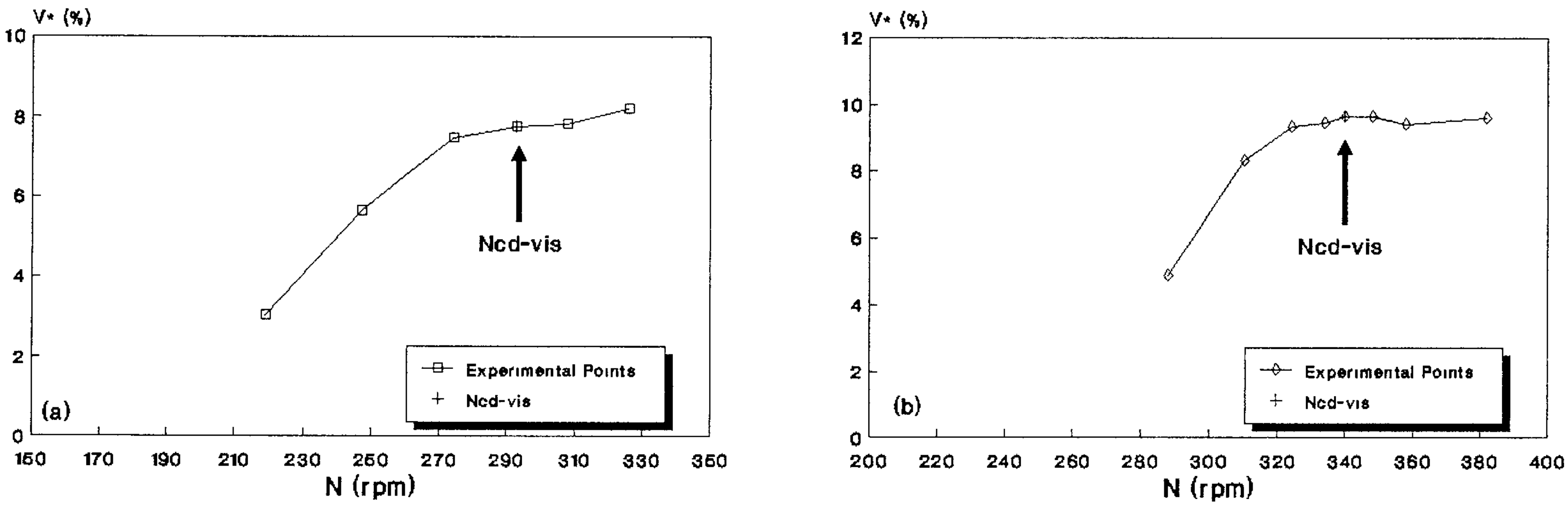
V* (%)
(a)
Ncd-vis
Experimental Points
Ncd-vis
N (rpm)
150 170 190 210 230 250 270 290 310 330 350
0 2 4 6 8 10
V* (%)
(b)
Ncd-vis
Experimental Points
Ncd-vis
N (rpm)
200 220 240 260 280 300 320 340 360 380 400
0 2 4 6 8 10 12

Figure 4.

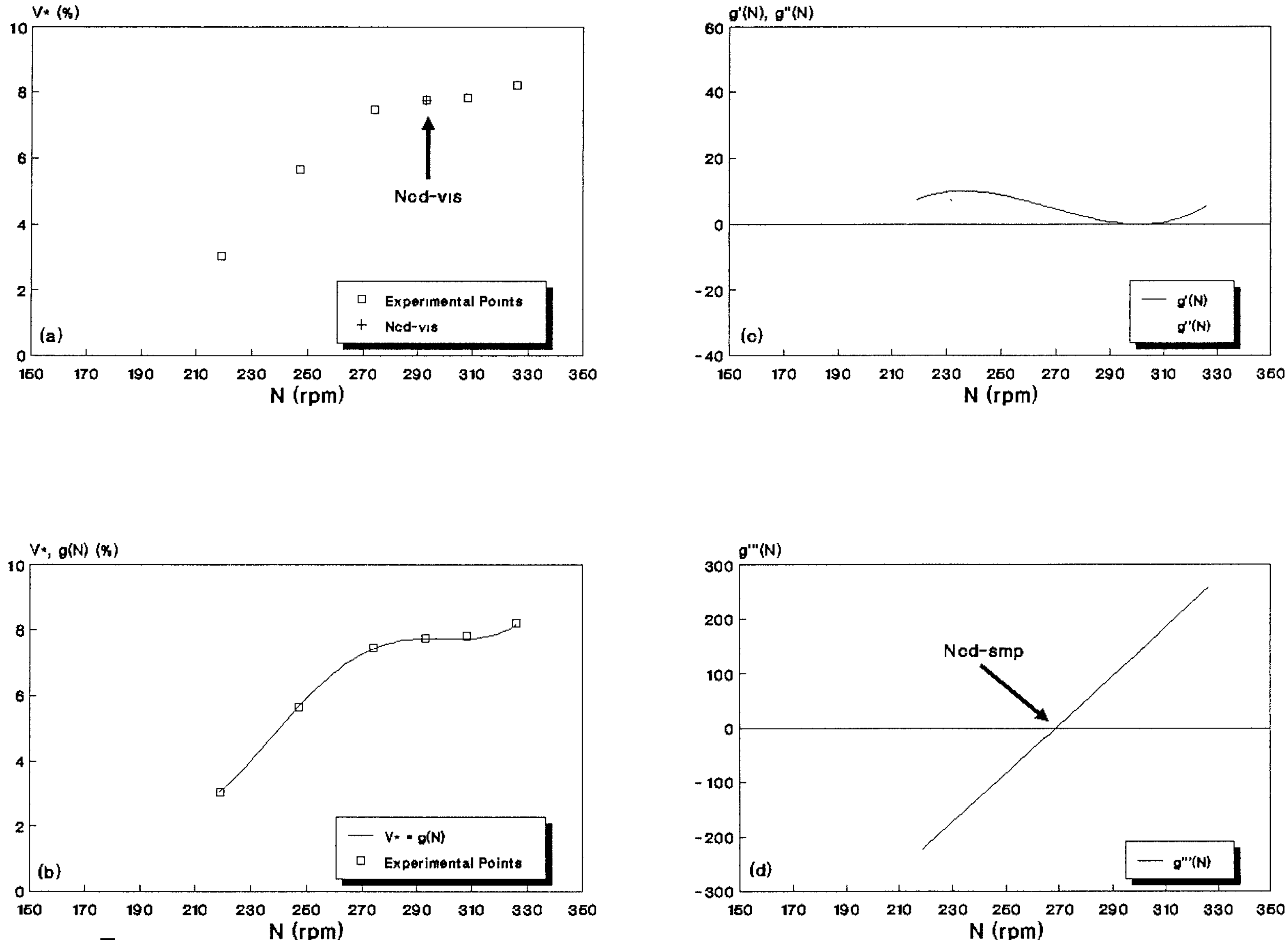

V* (%)
Ncd-vis
Experimental Points
Ncd-vis
(a)
N (rpm)
g'(N), g''(N)
g'(N)
g''(N)
(c)
N (rpm)
V*, g(N) (%)
V* = g(N)
Experimental Points
(b)
N (rpm)
g'''(N)
Ncd-smp
g'''(N)
(d)
N (rpm)

Figure 5.

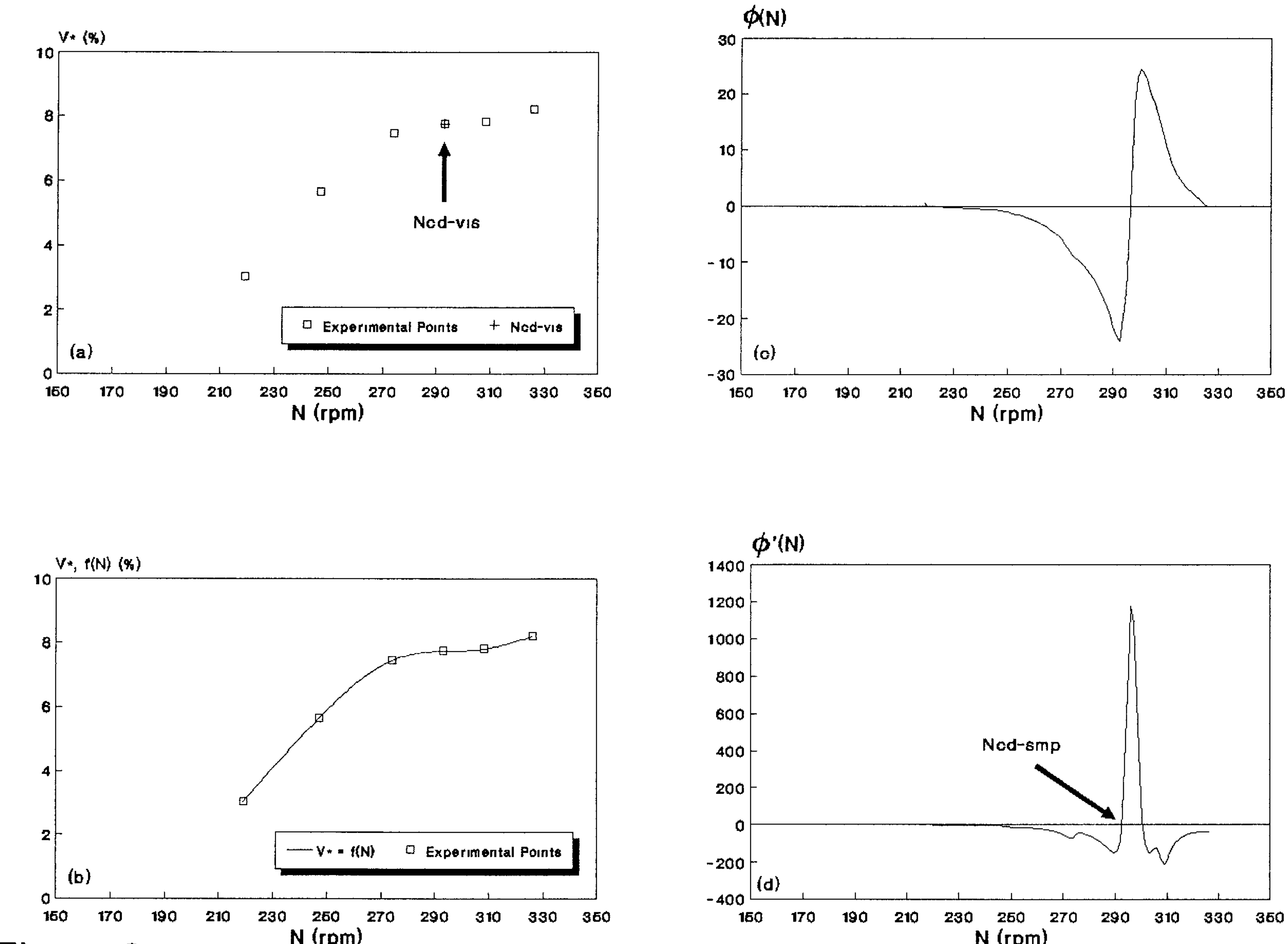

V* (%)
Ncd-vis
Experimental Points
Ncd-vis
(a)
N (rpm)
φ(N)
(c)
N (rpm)
V*, f(N) (%)
V* = f(N)
Experimental Points
(b)
N (rpm)
φ'(N)
Ncd-smp
(d)
N (rpm)

Figure 6.

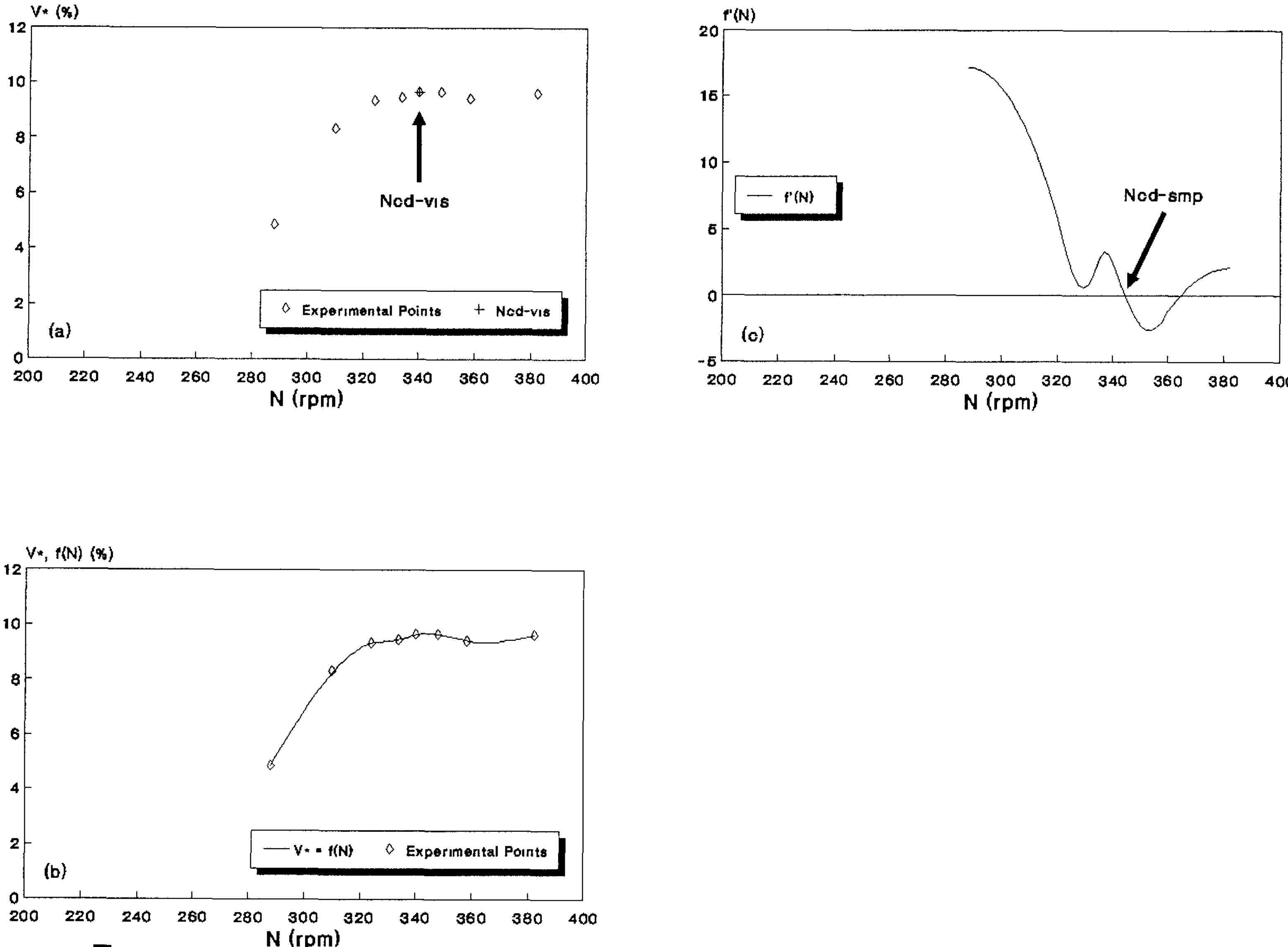
V* (%)
Ncd-vis
Experimental Points
Ncd-vis
(a)
N (rpm)
f'(N)
f'(N)
Ncd-smp
(c)
N (rpm)
V*, f(N) (%)
V* = f(N)
Experimental Points
(b)
N (rpm)

Figure 7.

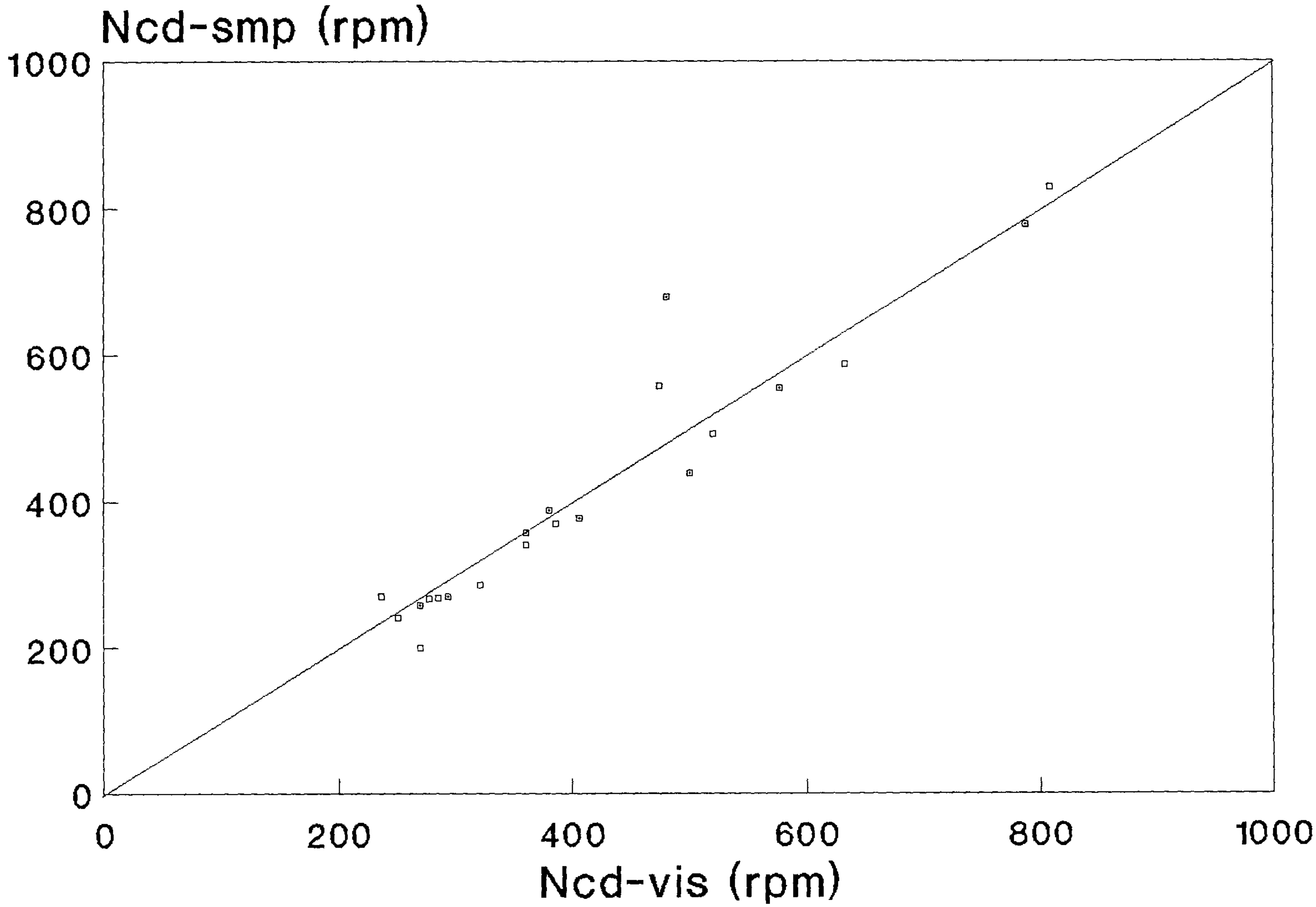
Ncd-smp (rpm)
1000
800
600
400
200
0
0
200
400
600
800
1000
Ncd-vis (rpm)

Figure 8.

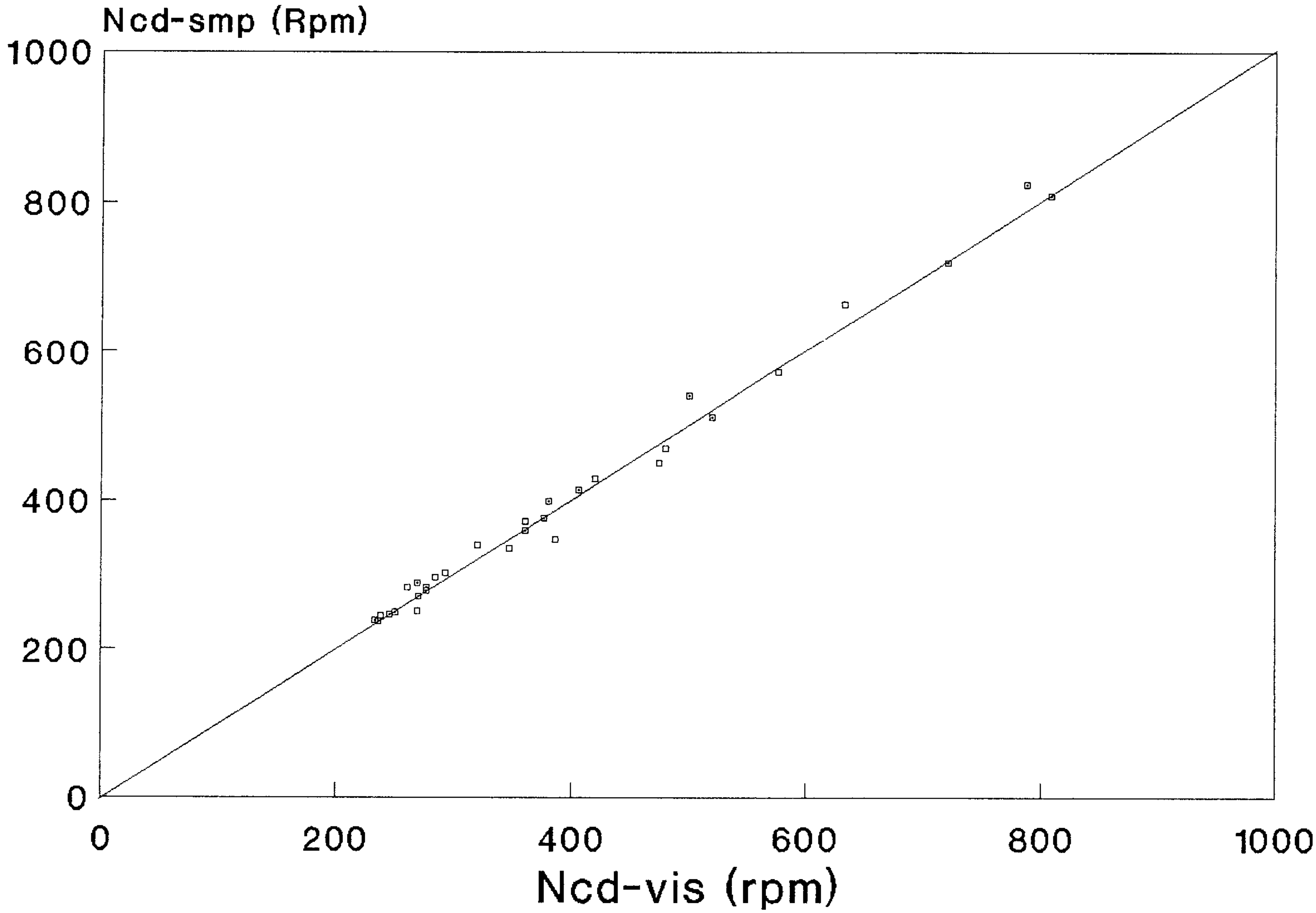
Ncd-smp (Rpm)
1000
800
600
400
200
0
0
200
400
600
800
1000
Ncd-vis (rpm)

Figure 9.

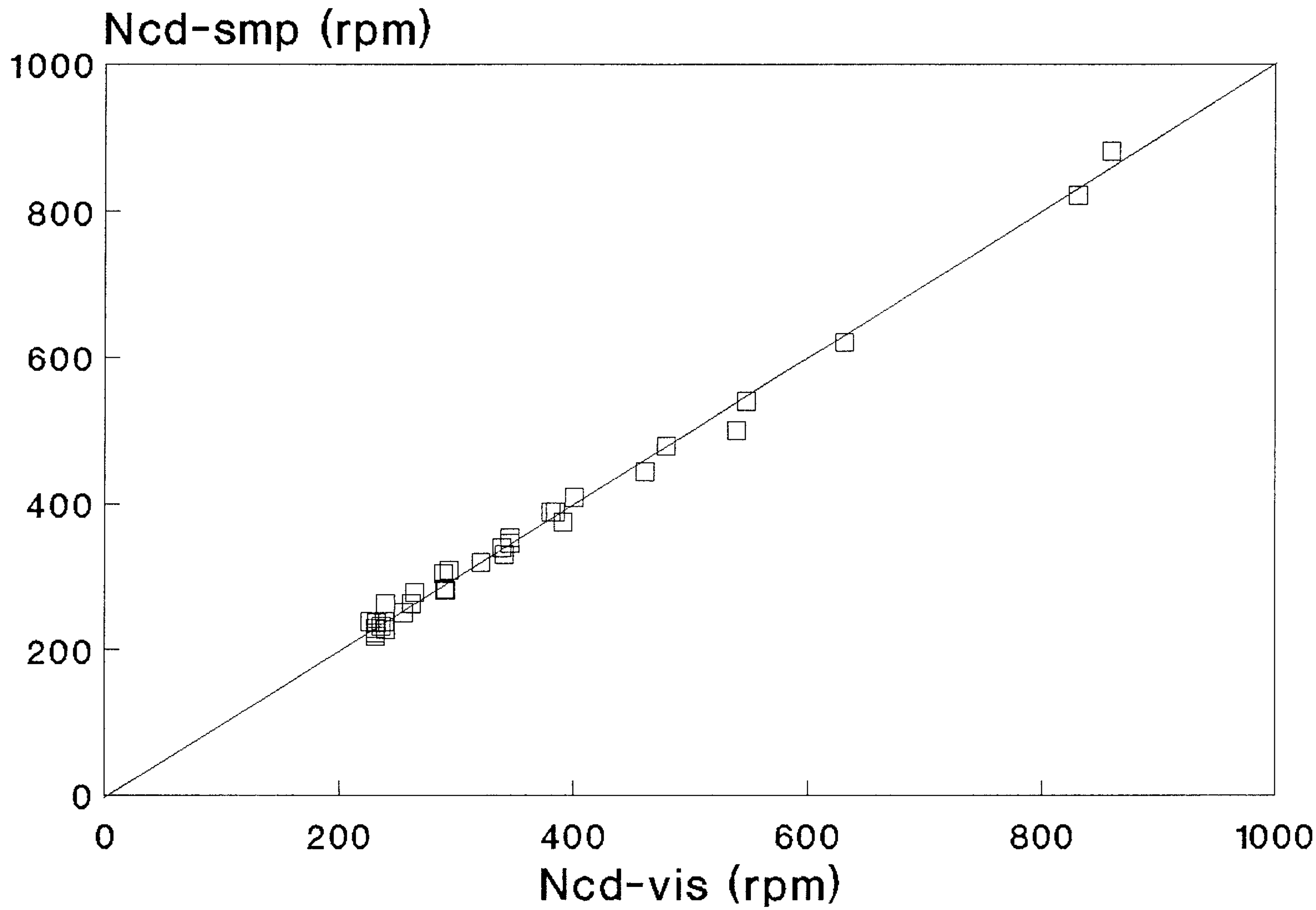
Ncd-smp (rpm)
1000
800
600
400
200
0
0
200
400
600
800
1000
Ncd-vis (rpm)

Figure 10.

43

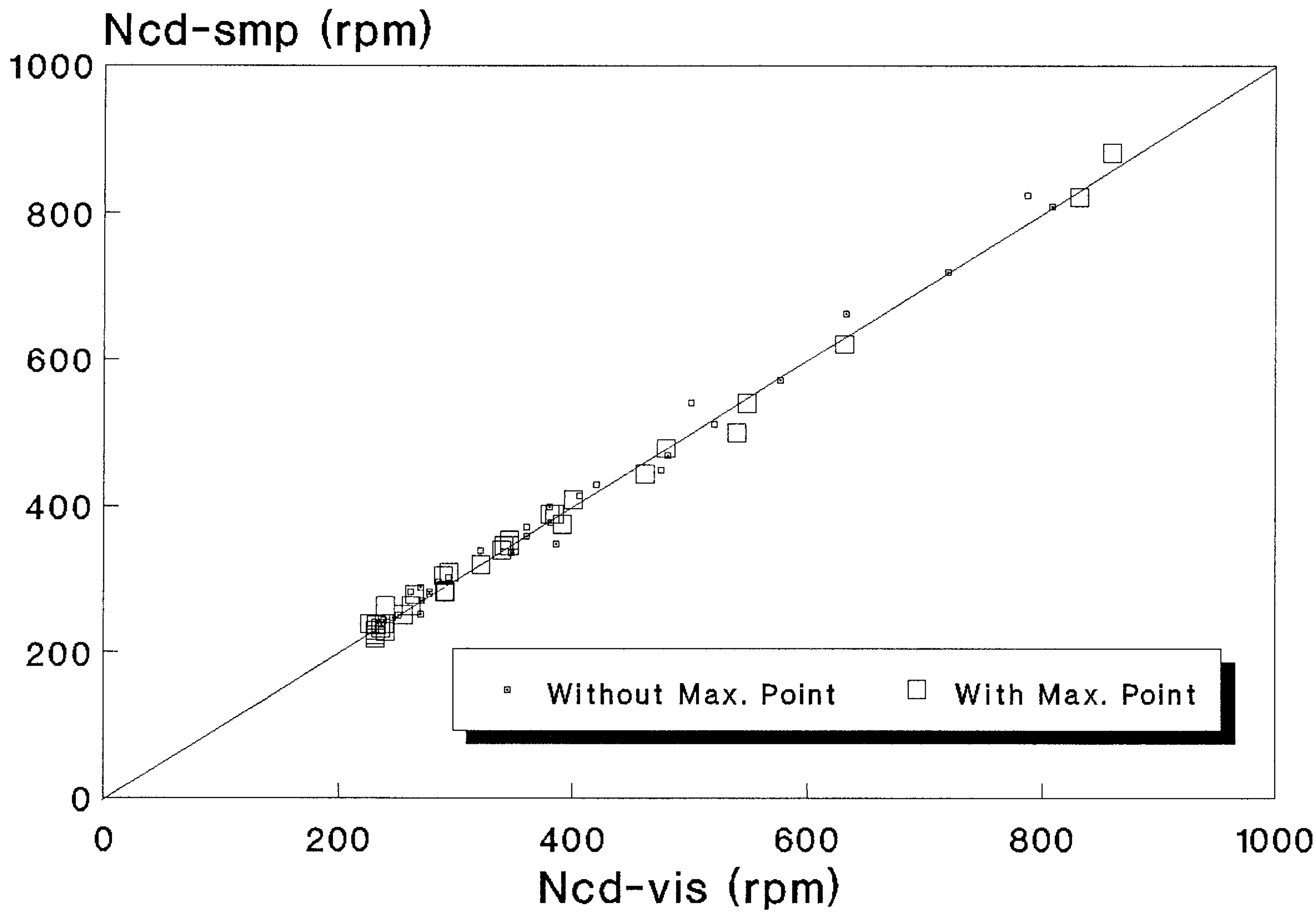

Ncd-smp (rpm)
1000
800
600
400
200
0
0
200
400
600
800
1000
Ncd-vis (rpm)
Without Max. Point
With Max. Point

Figure 11.

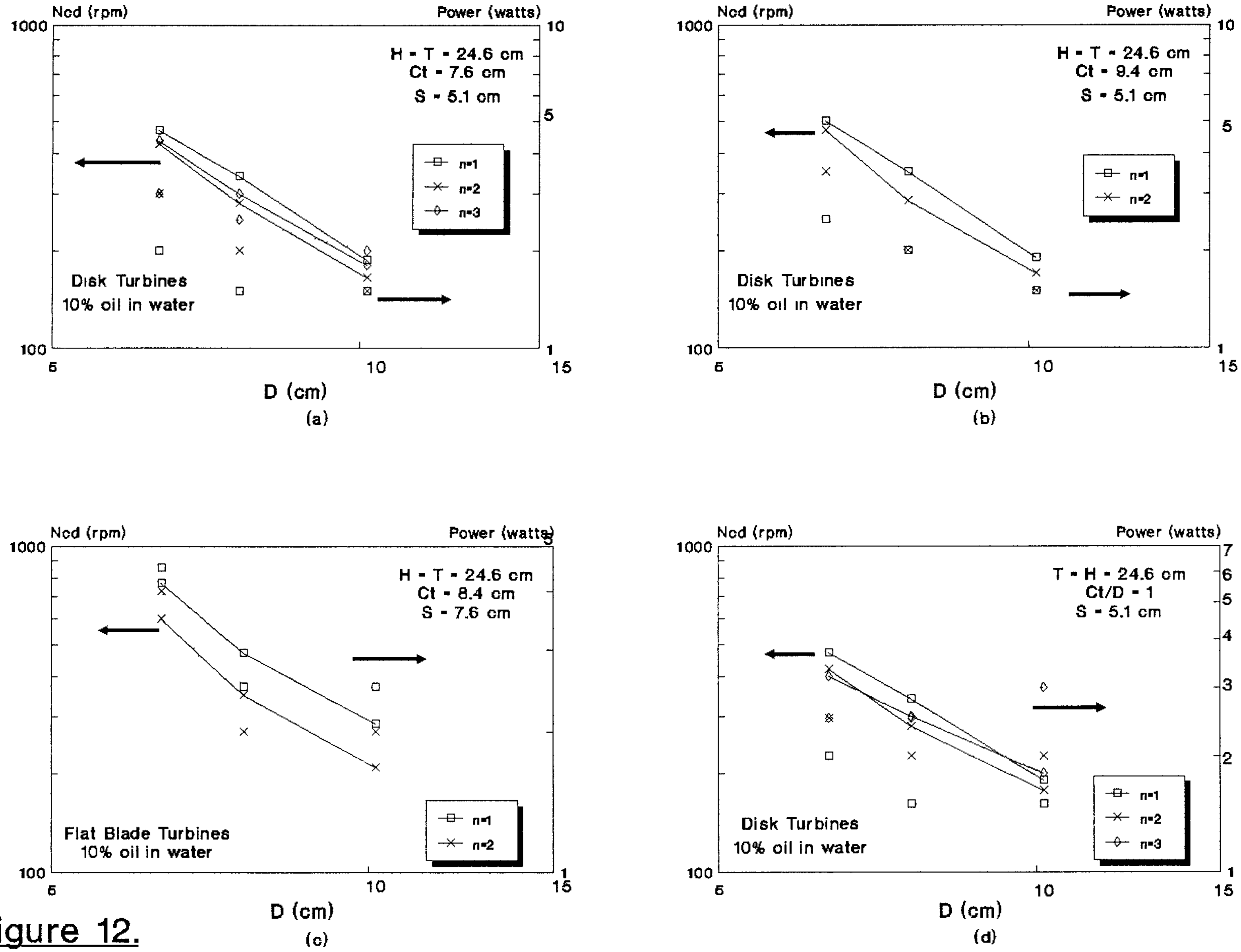
Ncd (rpm)
Power (watts)
H = T = 24.6 cm
Ct = 7.6 cm
S = 5.1 cm
n=1
n=2
n=3
Disk Turbines
10% oil in water
D (cm)
(a)
Ncd (rpm)
Power (watts)
H = T = 24.6 cm
Ct = 9.4 cm
S = 5.1 cm
n=1
n=2
Disk Turbines
10% oil in water
D (cm)
(b)
Ncd (rpm)
Power (watts)
H = T = 24.6 cm
Ct = 8.4 cm
S = 7.6 cm
n=1
n=2
Flat Blade Turbines
10% oil in water
D (cm)
(c)
Ncd (rpm)
Power (watts)
T = H = 24.6 cm
Ct/D = 1
S = 5.1 cm
n=1
n=2
n=3
Disk Turbines
10% oil in water
D (cm)
(d)

Figure 12.

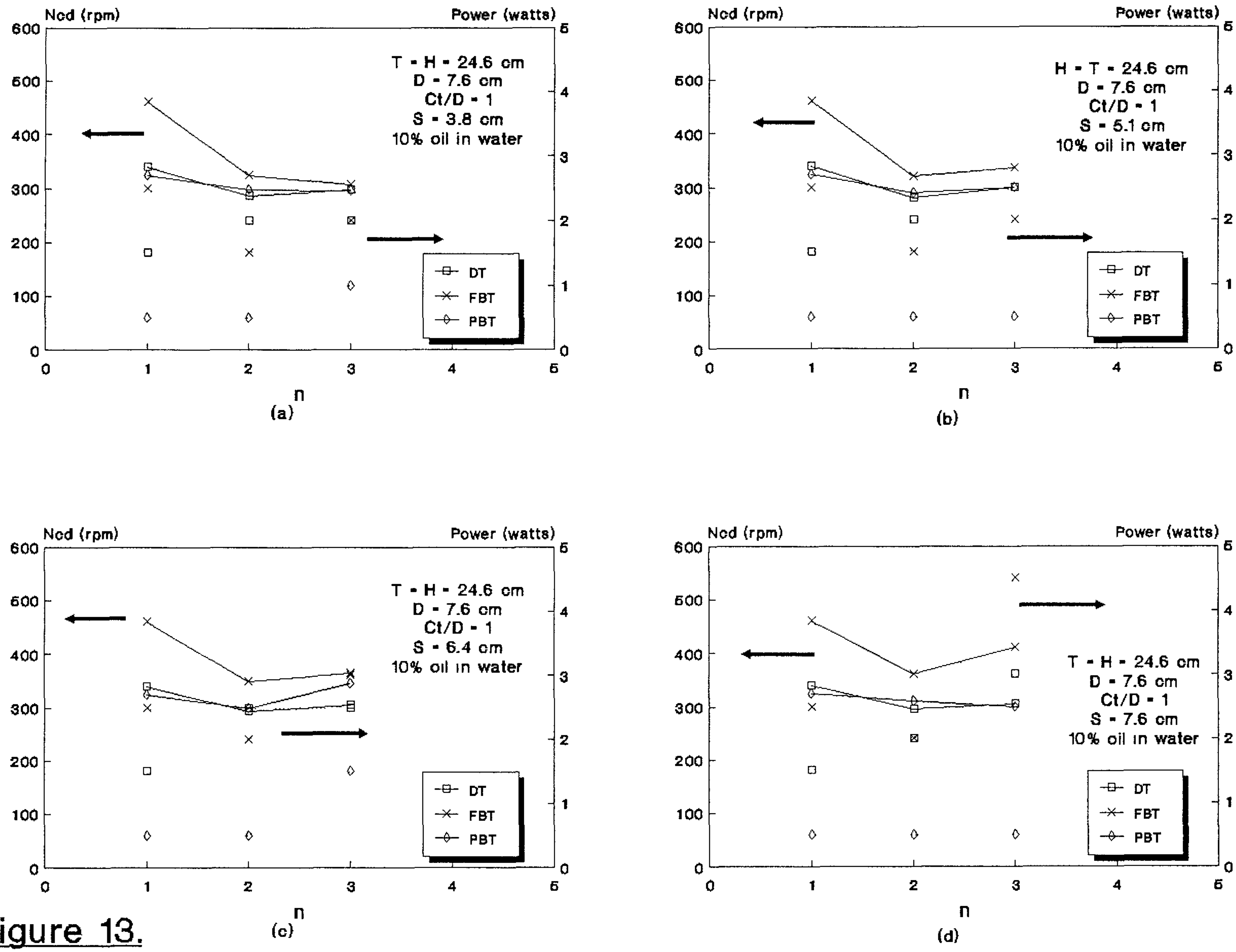

Ncd (rpm)
Power (watts)
T = H = 24.6 cm
D = 7.6 cm
Ct/D = 1
S = 3.8 cm
10% oil in water
DT
FBT
PBT
n
(a)
Ncd (rpm)
Power (watts)
H = T = 24.6 cm
D = 7.6 cm
Ct/D = 1
S = 5.1 cm
10% oil in water
DT
FBT
PBT
n
(b)
Ncd (rpm)
Power (watts)
T = H = 24.6 cm
D = 7.6 cm
Ct/D = 1
S = 6.4 cm
10% oil in water
DT
FBT
PBT
n
(c)
Ncd (rpm)
Power (watts)
T = H = 24.6 cm
D = 7.6 cm
Ct/D = 1
S = 7.6 cm
10% oil in water
DT
FBT
PBT
n
(d)

Figure 13.

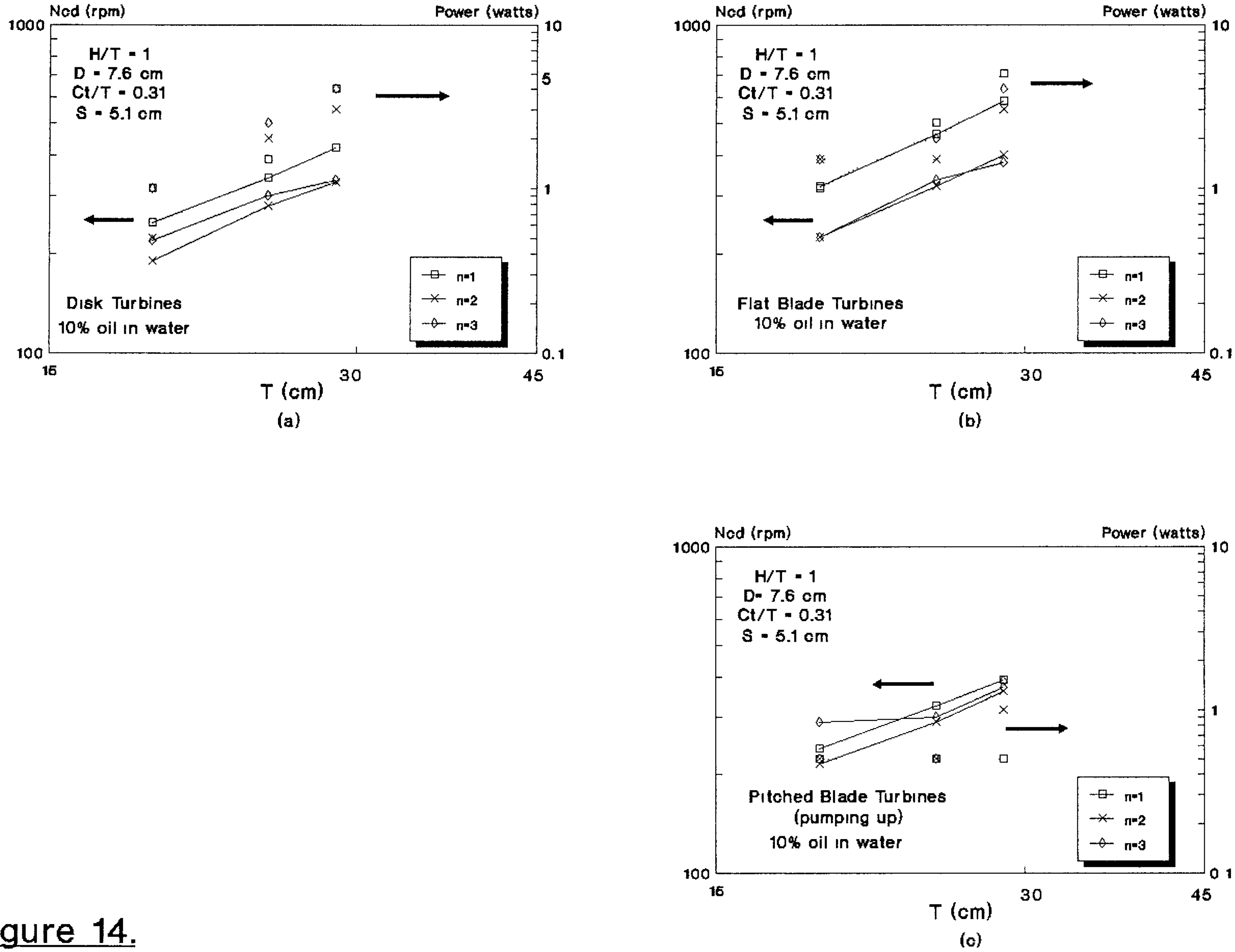
Ncd (rpm)
Power (watts)
H/T = 1
D = 7.6 cm
Ct/T = 0.31
S = 5.1 cm
Disk Turbines
10% oil in water
n=1
n=2
n=3
T (cm)
(a)
Flat Blade Turbines
10% oil in water
(b)
Pitched Blade Turbines
(pumping up)
10% oil in water
(c)

Figure 14.

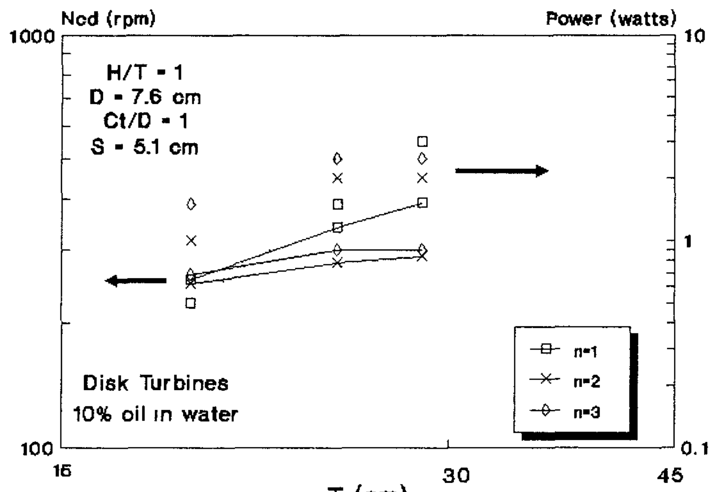

(a)

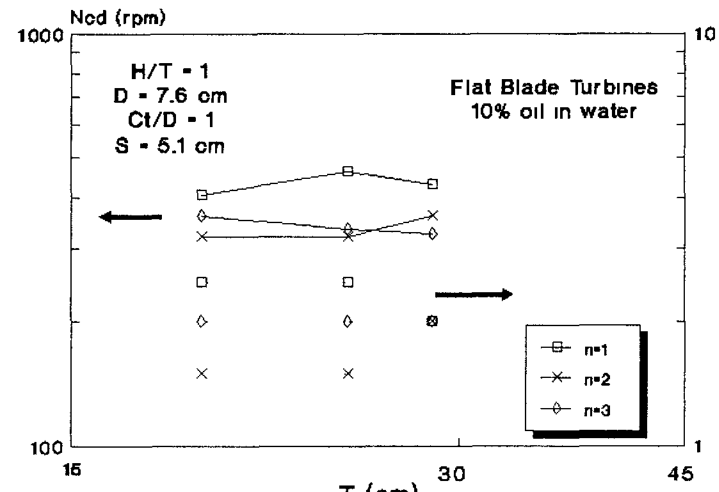

(b)

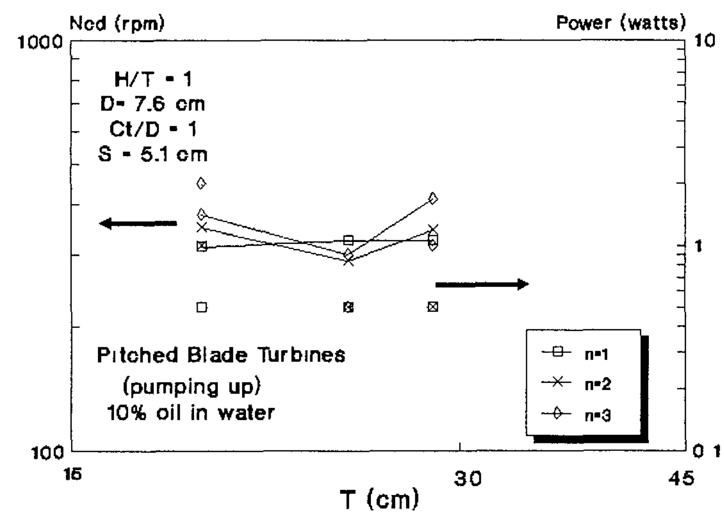

(c)

Figure 15.

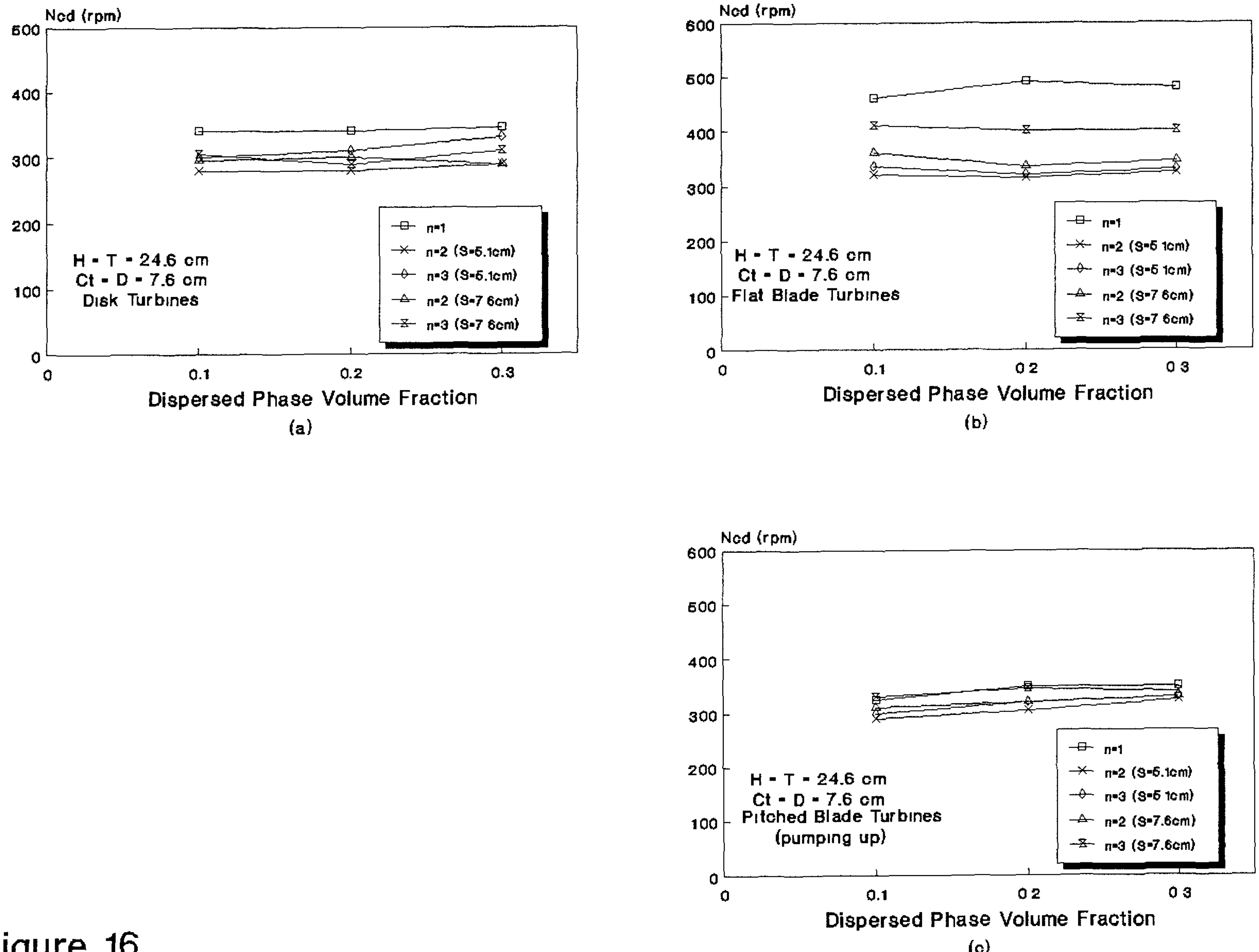

Ncd (rpm)
H - T - 24.6 cm
Ct - D - 7.6 cm
Disk Turbines
n=1
n=2 (S=5.1cm)
n=3 (S=5.1cm)
n=2 (S=7 6cm)
n=3 (S=7 6cm)
Dispersed Phase Volume Fraction
(a)
Ncd (rpm)
H - T - 24.6 cm
Ct - D - 7.6 cm
Flat Blade Turbines
n=1
n=2 (S=5 1cm)
n=3 (S=5 1cm)
n=2 (S=7 6cm)
n=3 (S=7 6cm)
Dispersed Phase Volume Fraction
(b)
Ncd (rpm)
H - T - 24.6 cm
Ct - D - 7.6 cm
Pitched Blade Turbines
(pumping up)
n=1
n=2 (S=5.1cm)
n=3 (S=5 1cm)
n=2 (S=7.6cm)
n=3 (S=7.6cm)
Dispersed Phase Volume Fraction
(c)

<u>Figure 16.</u>

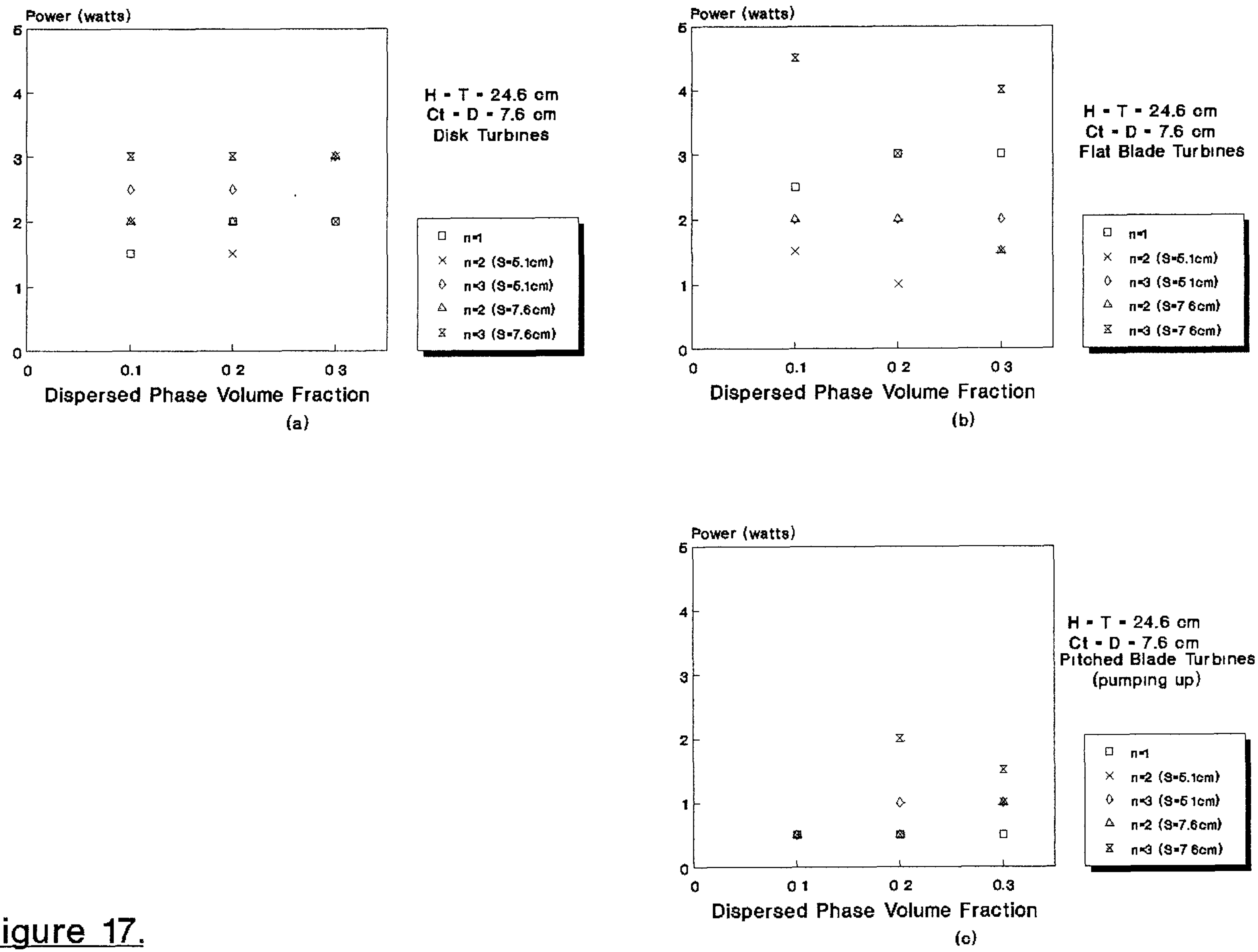
Power (watts)
Dispersed Phase Volume Fraction
(a)
H = T = 24.6 cm
Ct = D = 7.6 cm
Disk Turbines
n=1
n=2 (S=5.1cm)
n=3 (S=5.1cm)
n=2 (S=7.6cm)
n=3 (S=7.6cm)
Power (watts)
Dispersed Phase Volume Fraction
(b)
H = T = 24.6 cm
Ct = D = 7.6 cm
Flat Blade Turbines
n=1
n=2 (S=5.1cm)
n=3 (S=5.1cm)
n=2 (S=7.6cm)
n=3 (S=7.6cm)
Power (watts)
Dispersed Phase Volume Fraction
(c)
H = T = 24.6 cm
Ct = D = 7.6 cm
Pitched Blade Turbines
(pumping up)
n=1
n=2 (S=5.1cm)
n=3 (S=5.1cm)
n=2 (S=7.6cm)
n=3 (S=7.6cm)

Figure 17.

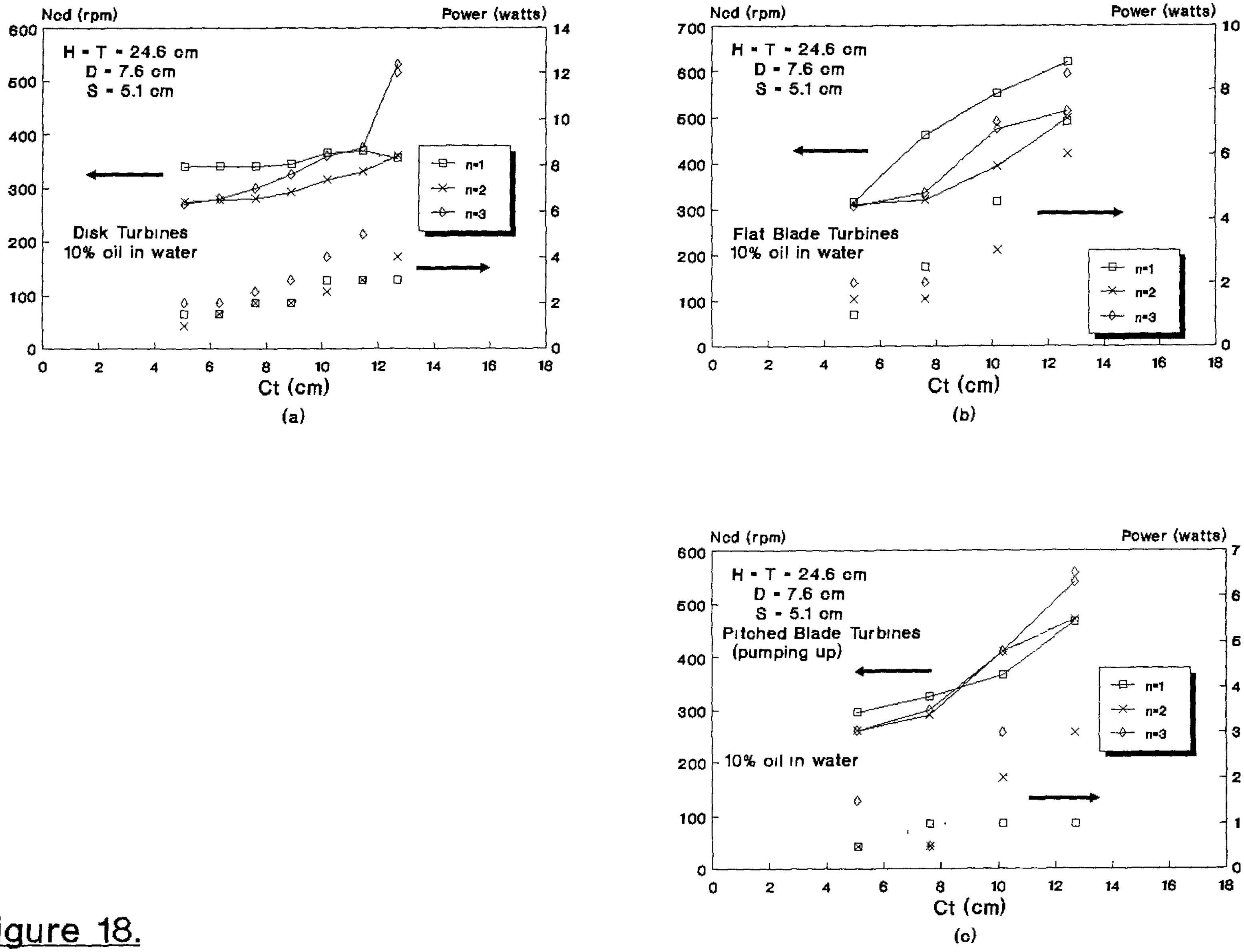

Ncd (rpm)
Power (watts)
H = T = 24.6 cm
D = 7.6 cm
S = 5.1 cm
Disk Turbines
10% oil in water
n=1
n=2
n=3
Ct (cm)
(a)
Ncd (rpm)
Power (watts)
H = T = 24.6 cm
D = 7.6 cm
S = 5.1 cm
Flat Blade Turbines
10% oil in water
n=1
n=2
n=3
Ct (cm)
(b)
Ncd (rpm)
Power (watts)
H = T = 24.6 cm
D = 7.6 cm
S = 5.1 cm
Pitched Blade Turbines
(pumping up)
10% oil in water
n=1
n=2
n=3
Ct (cm)
(c)

Figure 18.

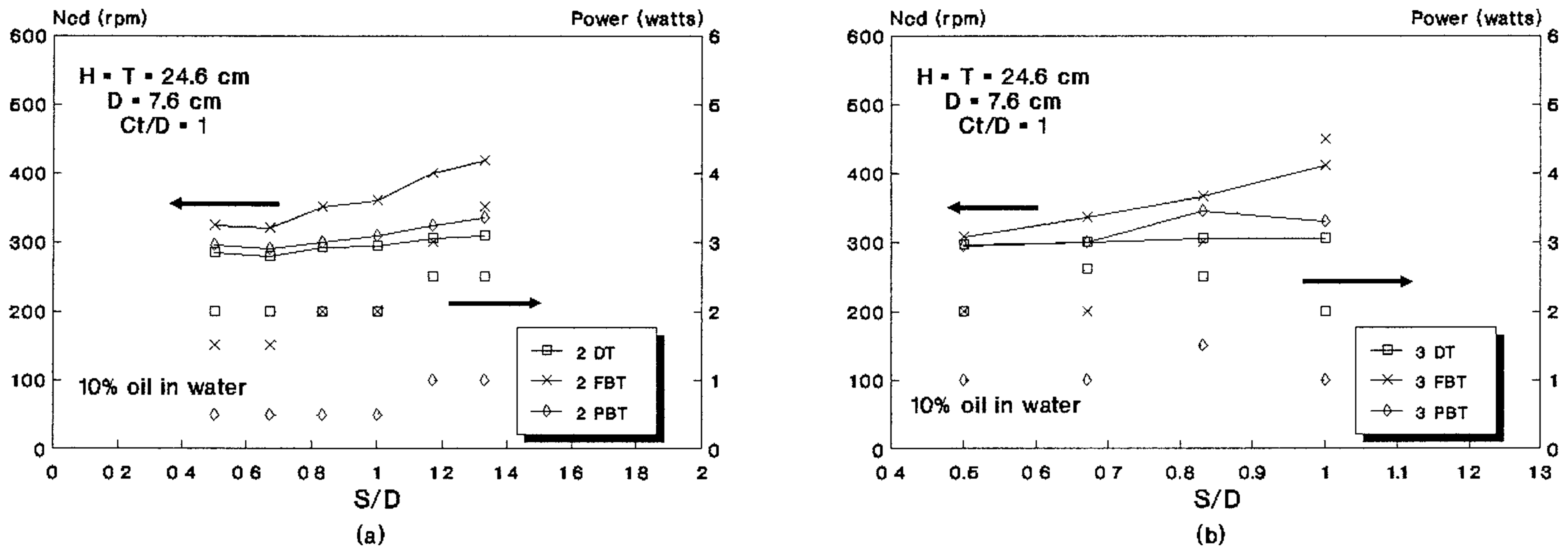

Ncd (rpm)
Power (watts)
H = T = 24.6 cm
D = 7.6 cm
Ct/D = 1
10% oil in water
2 DT
2 FBT
2 PBT
S/D
(a)
Ncd (rpm)
Power (watts)
H = T = 24.6 cm
D = 7.6 cm
Ct/D = 1
10% oil in water
3 DT
3 FBT
3 PBT
S/D
(b)

Figure 19.

Appendix

A. Data for Determination of the Minimum Agitation Speed

Case 1. The plot of the experimental value of V* vs N does not have any maxima

10% oil in water, H = T = 24.6 cm, D = 7.6 cm

type of impeller	n	Cb cm	sample location from bottom cm	Ncd-vis rpm	Ncd-smp by spline method rpm	Ncd-smp by polynomial method rpm
disk turbine	1	7.6	3.8	500	540	438
flat turbine	1	7.6	3.8	808	809	828
flat turbine	1	7.6	11.4	787	824	778
pitched blade turbine (pumping down)	1	7.6	3.8	633	663	586

10% heptane in water H = T = 28.6 cm, D = 7.6 cm

type of impeller	n	S cm	Cb cm	sample location from bottom cm	Ncd-vis rpm	Ncd-smp by spline method rpm	Ncd-smp by polynomial method rpm
disk turbine	2	10	10	15	381	376	
disk turbine	2	7.6	7.6	15	406	414	377
disk turbine	3	7.6	7.6	15	320	339	285
disk turbine	3	7.6	3.8	15	360	353	340
disk turbine	3	5	5	15	420	429	
disk turbine	3	5	8	15	380	398	387
flat blade turbine	2	7.6	7.6	15	520	511	491
flat blade turbine	2	7.6	15.2	15	360	371	357
flat blade turbine	3	7.6	3.8	15	480	469	680
flat blade turbine	3	3.8	3.8	15	720	720	

10% heptane in water, H = T = 28.6 cm, D = 10.2 cm

type of impeller	n	S cm	Cb cm	sample location from bottom cm	Ncd-vis rpm	Ncd-smp by spline method rpm	Ncd-smp by polynomial method rpm
disk turbine	1		10	10	277	282	
disk turbine	2	5	5	10	284	295	268
disk turbine	2	5	10	10	260	267	
disk turbine	2	10	5	10	269	251	257
disk turbine	2	5	8	10	277	278	266
disk turbine	3	5	5	10	269	288	199
disk turbine	3	5	8	10	253	242	
disk turbine	3	5	10	10	238	244	
disk turbine	3	7	5	10	250	249	241
disk turbine	3	7	8	10	233	239	
disk turbine	4	5	5	10	236	237	270
flat blade turbine	1		8.5	5.5	474	449	473
flat blade turbine	2	10	8.5	20	270	270	
flat blade turbine	2	5	8	10	347	335	
flat blade turbine	2	10	10	10	261	282	
flat blade turbine	2	10	8	10	293	293	269
flat blade turbine	2	10	5	10	386	347	369
pitched blade turbine (pumpıg down)	1		8.5	5.5	577	571	554

Case 2. The plot of the experimental values fo V* vs. N shows a maximum point

10% oil in water, H = T = 24.6 cm, D = 7.6 cm

type of impeller	n	S cm	Cb cm	sample location from bottom cm	Ncd-vis rpm	Ncd-smp by spline method rpm
disk turbine	1		7.6	11.4	390	374
disk turbine	1		10.2	3.8	345	329
disk turbine	1		10.2	11.4	340	344
flat blade turbine	1		10.2	11.4	859	881
flat blade turbine	1		10.2	3.81	830	820
pitched blade turbine (pumping down)	1		7.6	11.4	631	620
pitched blade turbine (pumping down)	1		10.2	11.4	539	499
pitched blade turbine (pumping down)	1		10.2	3.8	547	539
pitched blade turbine (pumping down)	2	7.6	7.6	11.4	345	352

10% heptane in water, H = T = 28.6 cm, D = 10.2 cm

type of impeller	n	S cm	Cb cm	sample location from bottom cm	Ncd-vis rpm	Ncd-smp by spline method rpm
disk turbine	1		8.5	15.5	288	303
disk turbine	1		8.5	5.5	289	280
disk turbine	1		7	10	320	319
disk turbine	1		8.5	20	290	280
disk turbine	2	10	8.5	15.5	231	235
disk turbine	2	10	8.5	5.5	235	231
disk turbine	2	10	8.5	20	230	228
disk turbine	2	10	8.5	20	230	222
disk turbine	2	10	8.5	20	230	218
disk turbine	2	7	5	20	293	307
disk turbine	2	7	8	10	254	250
disk turbine	2	7	10	10	239	262
disk turbine	2	10	8	10	239	226
disk turbine	2	10	10	10	226	238
disk turbine	4	5	8	10	238	238
flat blade turbine	2	10	8.5	5.5	261	262
flat blade turbine	2	10	8.5	15.5	264	277
flat blade turbine	2	5	10	10	289	282
flat blade turbine	2	7	8	10	338	338
pitched blade turbine (pumping up)	1		8.5	5.5	478	477

10% heptane in water, H = T = 28.6 cm, D = 7.6 cm

type of impeller	n	S cm	Cb cm	sample location from bottom cm	Ncd-vis rpm	Ncd-smp by spline method rpm
disk turbine	2	7.6	10	15	384	388
flat blade turbine	2	15.2	7.6	15	380	387
flat blade turbine	3	7.6	7.6	15	400	407
flat blade turbine	3	3.8	7.6	15	460	443

B. Data for Effect of Variables on Ncd and Power Consumption

1. Effect of impeller diameter

Disk turbine
10% oil in water , H = T = 24.6 cm, Ct = 7.6cm, S = 5.1 cm

	n = 1		n = 2		n = 3	
impeller diameter cm	Ncd rpm	power watts	Ncd rpm	power watts	Ncd rpm	power watts
6.4	470	2	425	3	435	3
7.6	340	1.5	280	2	300	2.5
10.2	187	1.5	165	1.5	180	2

The exponent value of D in Ncd vs D

impeller number	a	standard error	correlation coefficient
1	-1.97	0.166	-0.9991
2	-2.0	0.248	-0.9982
3	-1.87	0.144	-0.9993

Disk turbine
10% oil in water, H = T = 24.6 cm, Ct = 9.4 cm, S = 5.1 cm

	n = 1		n = 2	
impeller diameter cm	Ncd rpm	power watts	Ncd rpm	power watts
6.4	500	2.5	470	3.5
7.6	350	2	285	2
10.2	190	1.5	170	1.5

The exponent value of D in Ncd vs D

impeller number	a	standard error	correlation coefficient
1	-2.07	0.092	-0.9998
2	-2.13	0.522	-0.9929

Flat blade turbine
10% oil in water, H = T =24.6 cm, Ct = 8.4 cm, S = 7.6 cm

	n = 1		n = 2	
impeller diameter cm	Ncd rpm	power watts	Ncd rpm	power watts
6.4	770	4.5	600	4
7.6	470	2.5	350	2
10.2	285	2.5	210	2

The exponent value of D in Ncd vs D

impeller number	a	standard error	correlation coefficient
1	-2.08	0.533	-0.992
2	-2.19	0.65	-0.9896

Disk turbine
10% oil in water, H = T = 24.6 cm, Ct/D = 1, S = 5.1 cm

	n = 1		n = 2		n = 3	
impeller diameter cm	Ncd rpm	power watts	Ncd rpm	power watts	Ncd rpm	power watts
6.4	470	2	420	2.5	400	2.5
7.6	340	1.5	280	2	300	2.5
10.2	190	1.5	177	2	200	3

The exponent value of D in Ncd vs D

impeller number	a	standard error	correlation coefficient
1	-1.94	0.136	-0.9994
2	-1.82	0.347	-0.9957
3	-1.47	0.093	-0.9995

2.Effect of number of impellers

H = T = 24.6 cm, Ct/D =1, D = 7.6 cm, S = 3.8 cm
10% oil in water

	n = 1		n = 2		n = 3	
type of impeller	Ncd rpm	power watts	Ncd rpm	power watts	Ncd rpm	power watts
disk turbine	340	1.5	285	2	297	2
flat blade turbine	460	2.5	325	1.5	307	2
pitched blade turbine	325	0.5	297	0.5	295	1

H = T = 24.6 cm, Ct/D = 24.6 cm, D = 7.6 cm, S = 5.1 cm
10% oil in water

	n = 1		n = 2		n = 3	
type of impeller	Ncd rpm	power watts	Ncd rpm	power watts	Ncd rpm	power watts
disk turbine	340	1.5	280	2	300	2.5
flat blade turbine	460	2.5	320	1.5	335	2
pitched blade turbine	325	0.5	290	0.5	300	0.5

H = T = 24.6 cm, Ct/D =1, D = 7.6 cm, S = 6.4 cm
10% oil in water

	n = 1		n = 2		n = 3	
type of impeller	Ncd rpm	power watts	Ncd rpm	power watts	Ncd rpm	power watts
disk turbine	340	1.5	283	2	305	2.5
flat blade turbine	460	2.5	350	2	365	3
pitched blade turbine	325	0.5	300	0.5	345	1.5

H = T = 24.6 cm, Ct/D =1, D = 7.6 cm, S = 7.6 cm
10% oil in water

	n = 1		n = 2		n = 3	
type of impeller	Ncd rpm	power watts	Ncd rpm	power watts	Ncd rpm	power watts
disk turbine	340	1.5	295	2	306	3
flat blade turbine	460	2.5	360	2	410	4.5
pitched blade turbine	325	0.5	310	0.5	300	0.5

3. Effect of tank diameter

Case 1:.Ct/T is constant

Disk turbine
10% oil in water, H/T = 1, Ct/T = 0.31, D = 7.6 cm, S = 5.1 cm

	n = 1		n = 2		n = 3	
tank diameter cm	Ncd rpm	power watts	Ncd rpm	power watts	Ncd rpm	power watts
18.9	250	1	190	0.5	220	1
24.6	340	1.5	280	2	300	2.5
28.6	420	4	330	3	335	4

The exponent value of T in Ncd vs T

impeller number	a	standard error	correlation coefficient
1	1.24	0.126	0.9987
2	1.35	0.203	0.9973
3	1.03	0.237	0.9937

Flat blade turbine
10% oil in water, H/T = 1, Ct/T = 0.31, D = 7.6 cm, S = 5.1 cm

	n = 1		n = 2		n = 3	
tank diameter cm	Ncd rpm	power watts	Ncd rpm	power watts	Ncd rpm	power watts
18.9	320	1	225	1.5	225	1.5
24.6	460	2.5	320	1.5	335	2
28.6	580	5	400	3	380	4

The exponent value of T in Ncd vs T

impeller number	a	standard error	correlation coefficient
1	1.45	0.116	0.9992
2	1.38	0.077	0.9996
3	1.29	0.359	0.9909

Pitched blade turbine

10% oil in water, H/T = 1, Ct/T = 0.31, D = 7.6 cm, S = 5.1 cm

	n = 1		n = 2		n = 3	
tank diameter cm	Ncd rpm	power watts	Ncd rpm	power watts	Ncd rpm	power watts
18.9	240	0.5	215	0.5	290	0.5
24.6	325	0.5	290	0.5	300	0.5
28.6	390	0.5	360	1	370	1.5

The exponent value of T in Ncd vs T

impeller number	a	standard error	correlation coefficient
1	1.17	0.032	0.9999
2	1.23	0.16	0.998
3	0.54	0.673	0.852

Case 2: Ct/D is constant

Disk turbine

10% oil in water, H/T = 1, Ct/D = 1, D = 7.6 cm, S = 5.1 cm

	n = 1		n = 2		n = 3	
tank diameter cm	Ncd rpm	power watts	Ncd rpm	power watts	Ncd rpm	power watts
18.9	255	0.5	250	1	262	1.5
24.6	340	1.5	280	2	300	2.5
28.6	390	3	290	2	300	2.5

The exponent value of T in Ncd vs T

impeller number	a	standard error	correlation coefficient
1	1.033	0.096	0.999
2	0.366	0.105	0.990
3	0.368	0.289	0.933

Flat blade turbine

10% oil in water, H/T = 1, Ct/D = 1, D = 7.6 cm, S = 5.1 cm

	n = 1		n = 2		n = 3	
tank diameter cm	Ncd rpm	power watts	Ncd rpm	power watts	Ncd rpm	power watts
18.9	405	2.5	322	1.5	360	2
24.6	460	2.5	320	1.5	335	2
28.6	430	2	360	2	325	2

The exponent value of T in Ncd vs T

impeller number	a	standard error	correlation coefficient
1	0.183	0.496	0.602
2	0.236	0.429	0.7474
3	-0.250	0.038	-0.9972

Pitched blade turbine

10% oil in water, H/T = 1, Ct/D = 1, D = 7.6 cm, S = 5.1 cm

	n = 1		n = 2		n = 3	
tank diameter cm	Ncd rpm	power watts	Ncd rpm	power watts	Ncd rpm	power watts
18.9	315	0.5	350	1	375	2
24.6	325	0.5	290	0.5	300	0.5
28.6	325	0.5	345	0.5	410	1

The exponent value of T in Ncd vs T

impeller number	a	standard error	correlation coefficient
1	0.08	0.063	0.9332
2	-0.11	0.994	-0.223
3	0.10	1.555	0.1245

4. Effect of the dispersed phase volume fraction ϕ

Disk turbine
H= T= 24.6 cm, Ct/D = 1, D = 7.6 cm, S = 5.1 cm

	n = 1		n = 2		n = 3	
volume fraction f	Ncd rpm	power watts	Ncd rpm	power watts	Ncd rpm	power watts
0.1	340	1.5	280	2	300	2.5
0.2	340	2	280	1.5	320	2.5
0.3	345	2	290	3	330	3

The exponent value of f in Ncd vs f

impeller number	a	standard error	correlation coefficient
1	0.01	0.019	0.7816
2	0.03	0.046	0.7816
3	0.09	0.009	0.9987

Disk turbine
H= T= 24.6 cm, Ct/D = 1, S/D = 1, D = 7.6 cm

	n = 2		n = 3	
volume fraction f	Ncd rpm	power watts	Ncd rpm	power watts
0.1	295	2	306	3
0.2	300	2	290	3
0.3	290	3	310	2

The exponent value of f in Ncd vs f

impeller number	a	standard error	correlation coefficient
2	-0.01	0.058	-0.3695
3	0.002	0.13	0.0346

Flat blade turbine
H= T= 24.6 cm, Ct/D = 1, D = 7.6 cm, S = 5.1 cm

	n = 1		n = 2		n = 3	
volume fraction f	Ncd rpm	power watts	Ncd rpm	power watts	Ncd rpm	power watts
0.1	460	2.5	320	1.5	335	2
0.2	490	3	315	1	320	2
0.3	480	3	325	1.5	330	2

The exponent value of f in Ncd vs f

impeller number	a	standard error	correlation coefficient
1	0.04	0.076	0.7653
2	0.01	0.054	0.3607
3	-0.02	0.076	-0.4599

Flat blade turbine
H= T= 24.6 cm, Ct/D = 1, S/D = 1, D = 7.6 cm

	n = 2		n = 3	
volume fraction f	Ncd rpm	power watts	Ncd rpm	power watts
0.1	360	2	410	4.5
0.2	335	2	400	3
0.3	345	1.5	400	4

The exponent value of f in Ncd vs f

impeller number	a	standard error	correlation coefficient
2	-0.05	0.095	-0.702
3	0.02	0.019	-0.931

Pitched blade turbine

H= T= 24.6 cm, Ct/D = 1, D = 7.6 cm, S = 5.1 cm

	n = 1		n = 2		n = 3	
volume fraction f	Ncd rpm	power watts	Ncd rpm	power watts	Ncd rpm	power watts
0.1	325	0.5	290	0.5	300	0.5
0.2	350	0.5	305	0.5	320	1
0.3	350	0.5	325	1	330	1

The exponent value of f in Ncd vs f

impeller number	a	standard error	correlation coefficient
1	0.07	0.057	0.9310
2	0.10	0.045	0.9767
3	0.09	0.009	0.9987

Pitched blade turbine

H= T= 24.6 cm, Ct/D = 1, S/D = 1, D = 7.6 cm

10% oil in water

	n = 2		n = 3	
volume fraction f	Ncd rpm	power watts	Ncd rpm	power watts
0.1	310	0.5	300	0.5
0.2	320	0.5	345	2
0.3	330	1	340	1.5

The exponent value of f in Ncd vs f

impeller number	a	standard error	correlation coefficient
2	0.06	0.016	0.99
3	0.12	0.128	0.9822

5. Effect of clearance distance

Disk turbine
H= T= 24.6 cm, D = 7.6 cm, S = 5.1 cm
10% oil in water

number of impeller	n = 1		n = 2		n=3	
clearance cm	Ncd rpm	power watts	Ncd rpm	power watts	Ncd rpm	power watts
5.1	340	1.5	275	1	270	2
6.4	340	1.5	278	1.5	280	2
7.6	340	2	280	2	300	2.5
8.9	345	2	292	2	325	3
10.2	365	3	315	2.5	360	4
11.4	370	3	330	3	375	5
12.7	355	3	360	4	530	12

Flat blade turbine
H= T= 24.6 cm, D = 7.6 cm, S = 5.1 cm
10% oil in water

number of impeller	n = 1		n = 2		n=3	
clearance cm	Ncd rpm	power watts	Ncd rpm	power watts	Ncd rpm	power watts
5.1	315	1	310	1.5	307	2
7.6	460	2.5	320	1.5	335	2
10.2	550	4.5	393	3	475	7
12.7	620	7	496	6	512	8.5

Pitched blade turbine
H= T= 24.6 cm, D = 7.6 cm, S = 5.1 cm
10% oil in water

number of impeller	n = 1		n = 2		n=3	
clearance cm	Ncd rpm	power watts	Ncd rpm	power watts	Ncd rpm	power watts
5.1	295	0.5	260	0.5	260	1.5
7.6	325	1	290	0.5	300	0.5
10.2	365	1	410	2	410	3
12.7	467	1	470	3	540	6.5

6.Effect of spacing between impellers

impeller number: 2
H= T= 24.6 cm, Ct/D = 1, D = 7.6 cm
10% oil in water

	disk turbine		flat blade turbine		pitched blade turbine	
spacing cm	Ncd rpm	power watts	Ncd rpm	power watts	Ncd rpm	power watts
3.8	285	2	325	1.5	297	0.5
5.1	280	2	320	1.5	290	0.5
6.4	293	2	350	2	300	0.5
7.6	295	2	360	2	310	0.5
8.9	306	2.5	400	3	325	1
10.2	310	2.5	417	3.5	335	1

The exponent value of in Ncd vs S

type of impeller	a	standard error	correlation coefficient
disk turbine	0.10	0.046	0.9065
flat blade turbine	0.27	0.11	0.9309
pitched blade turbine	0.14	0.073	0.882

impeller number: 3
H= T= 24.6 cm, Ct/D = 1, D = 7.6 cm
10% oil in water

	disk turbine		flat blade turbine		pitched blade turbine	
spacing cm	Ncd rpm	power watts	Ncd rpm	power watts	Ncd rpm	power watts
3.8	296	2	307	2	295	1
5.1	300	2.5	335	2	300	1
6.4	305	2.5	365	3	345	1.5
7.6	306	2	410	4.5	330	1

The exponent value of in Ncd vs S

type of impeller	a	standard error	correlation coefficient
disk turbine	0.05	0.013	0.9806
flat blade turbine	0.41	0.102	0.9854
pitched blade turbine	0.21	0.203	0.8304